Geology of Nisyros Volcano

3

Volker Jörg Dietrich

Abstract

The heart of the book is found in this Chapter, the geology of Nisyros Volcano. The compilation of the new "Geological Map of the Island of Nisyros (Dodecanese Archipelago)" with cross sections serves as the basis for the interpretation of the eruptive history of Nisyros volcano. The volcano-tectonic structures of the 698 m high stratovolcano are marked by the central, almost circular caldera with a diameter of 3.6 km and a drop of 300–400m of its steep walls. This dominant structural feature is crosscut by two conjugate major and three minor fault systems. Since accurate geochronological data are still missing due to the rarity of potassium bearing minerals, such as sanidine and biotite as well as to other petrologic and chemical reasons, the eruptive history can only be based on relative ages of a detailed lithostratigraphy of thirty-two mappable eruptive units. A major division into five volcanic cycles has been devised using eruptive successions, contact relationships, epiclastic deposits and intercalated paleosols. Volcanic activity started with shallow submarine basaltic-andesitic lavas during the "Early Shield Volcano Cycles" evolving into a subaerial environment with local lacustrine lakes. Progressively, a composite stratovolcano built up the circular shape of Nisyros Island, with eruptions on the northern and southern part of the island, the latter with effusion of rhyolitic lava. Along the east coast, mainly explosive eruptions

Electronic supplementary material The online version of this chapter (doi:10.1007/978-3-319-55460-0_3) contains supplementary material, which is available to authorized users.

V.J. Dietrich (✉)
Institute of Geochemistry and Petrology, Swiss Federal Institute of Technology, ETH Zurich, ETH-Zentrum, CH 8092 Zürich, Switzerland
e-mail: volker.dietrich@erdw.ethz.ch

V.J. Dietrich and E. Lagios (eds.), *Nisyros Volcano*, Active Volcanoes of the World,
DOI 10.1007/978-3-319-55460-0_3

produced two larger tuff cones of andesitic and dacitic compositions. During an evolved stratovolcanic stage, basaltic-andesites and andesites were emitted as lavas and pyroclastics from several smaller cinder, spatter and scoria cones covering the southern, western and northern slopes of the island. The "Composite Stratovolcanic Cycles" ended with the effusion of a large dacitic dome in the northern part of the island, which generated a major dome collapse of the northern slopes into the sea. With an unknown time gap, voluminous eruptions of rhyolitic pyroclastics started from the northern and southern eruptive centers, "Caldera Eruptive Cycles", followed by a first caldera collapse and successive voluminous rhyolitic lava flows, which extruded towards southeast. The youngest major explosive rhyolitic eruption occurred after an unknown time interval from a northern centre, covering the northern and eastern slopes with major pumice deposits and inducing a second-stage of the caldera collapse. Afterwards, during the "Post Caldera Eruptive Cycle", voluminous effusions of rhyodacitic magma filled the western part of the caldera with large domes and flows that extend towards the sea, in the southwest. Since then, Nisyros Volcano remains in a dormant stage. Magmatic counterparts, such as gabbroic and dioritic intrusives, as well as mafic cumulates have generated a large hydrothermal system at depth, which is still highly active today.

3.1 The Geological Map of the Island of Nisyros (Dodecanese Archipelago) (1:15,000 with Geological Cross Sections)

The first geographic and geological studies on Nisyros Island were undertaken by the Italian geologists Martelli (1917), Chap. 5.2, Fig. 5.4 and Desio (1931). Detailed geological investigations started in the late sixtieth (Davis 1967), followed by Di Paola (1974), and Papanikolaou et al. (1991) with geological sketch maps at various scales. Vougioukalakis (1993) presented the first geological map of Nisyros Island on a topographic base in the scale of 1:12,500, which was updated in the Sheet Nisyros, Geological Map of Greece, 1:25,000 (2003) by IGME (Institute of Geology and Mineral Exploration, Athens, Greece).

During the GEOWARN—IST 12310 project (2003) a Topographic and a Geological Map of Nisyros in the scale 1:10,000 with equidistance 10 m contour lines resulted using a completely new digital technology. As basis served an orthorectified 3D IKONOS-2 satellite image from Nisyros volcanic island (2000) with a 1 m resolution on ground, cartographic field mapping and extraction from the topographical map 1:50,000 (Hellenic Military Geographical Service 1972). This work was done by the Institute of Cartography and Geoinformation, Department of Civil, Environmental and Geomatic Engineering, Swiss Federal Institute of Technology, Zurich, Switzerland. The detailed Geological Map of Nisyros Volcano 1:12,500 by Volentik et al. (2005) was the first result of the accurate topography.

The current updated digital and fully vectorised version of the "Geological Map of the Island of Nisyros (Dodecanese Archipelago) 1:15,000 with Geological Cross Sections" represents a compilation of all available former geological data, as well as unpublished results of field mapping during the periods 2000–2003, 2010–2015. The online version of the "Geological Map of the Island of Nisyros (Dodecanese Archipelago)" 1:15,000 with "Geological Cross Sections" as well as

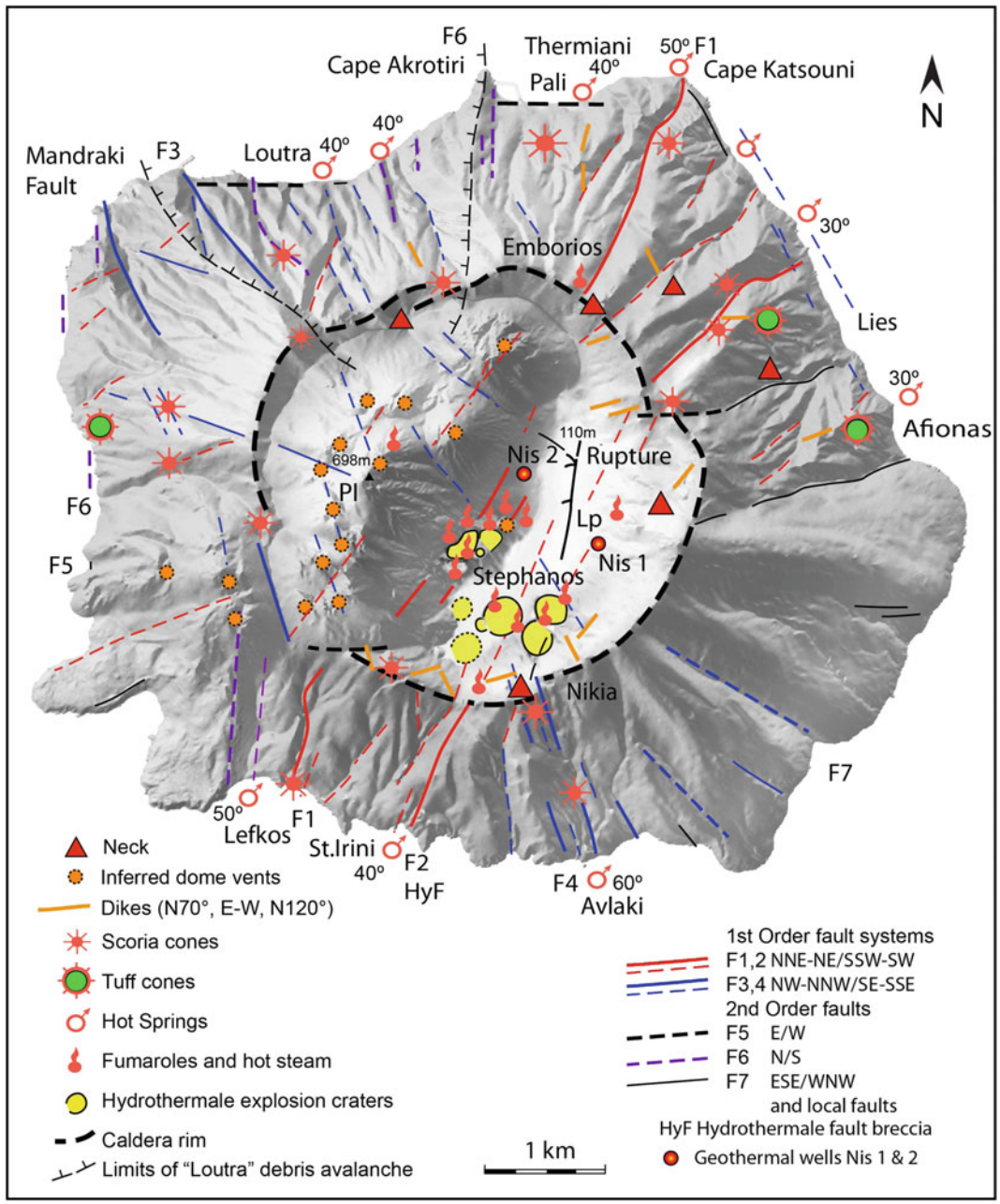

Fig. 3.1 The present-day structural map of Nisyros volcano deduced from the digital elevation model (*DEM*) of Nisyros Island, has been derived by digitizing the 1:5000 scale topographic map sheets of Nisyros Island, 1983, published by the Hellenic Military Geographical Service, Greece

detailed descriptions of the lithostratigrapjic units to Chap. 3 are available to authorized users.

Lithostratigraphic units (LSU) with numbers from 1 (lower most outcropping rocks on the island) to 33 (upper most or bounded with unconformity rocks) were used to designate mappable lavas and pyroclastic sequences. The numbering system of the units bears the advantage to the reader to recognize immediately their stratigraphic position. Local names and

abbreviations were restricted to a minimum to avoid confusion. On Nisyros Island the same or similar names occur for different localities and have changed throughout time. The grouping and division of units into cycles is based on unconformities, erosional surfaces, interbedded soils and epiclastic deposits.

The map is compatible with the *Hellenic Geodetic Reference System GGRS 87*, *Datum WGS 84* and the *Projection UTM Zone 35N (24E–30E)*. All geographic features are updated to 2015.

3.2 Volcanic and Volcano-Tectonic Structures

The present-day structural map of Nisyros volcano (Fig. 3.1) comprises volcanic eruption vents, such as necks, inferred dome vents, scoria cones (spatter and cinder cones included), tuff cones and sub-volcanic dikes, as well as hydrothermal explosion craters and emission spots: fumaroles, hot steam, and hot springs.

3.2.1 The Caldera

The most characteristic and dominant structural feature of Nisyros volcano is the caldera with an approximate diameter of 3.6 km (Fig. 3.2). The assumption of its post eruptive collapse origin led no doubts to all precious workers (see introduction) due to its almost circular structure and steep walls with a drop of 300–400 m between the northern and eastern rim down to the Lakki plain of 110 m a.s.l and to the filling of the western part with voluminous rhyodacitic domes up to 698 m. After the recognition of the two

Fig. 3.2 Aerial view of Nisyros volcano from northeast; the caldera with an approximate diameter of 3.6 km the filling of the western part with voluminous rhyodacitic domes up to 698 m (Profitis Ilias); the almost circular structure and steep walls with a drop of 300–400 m between the northern and eastern rim down to the Lakki plain of 110 m above sea level. *Photo* hellasmounts.com

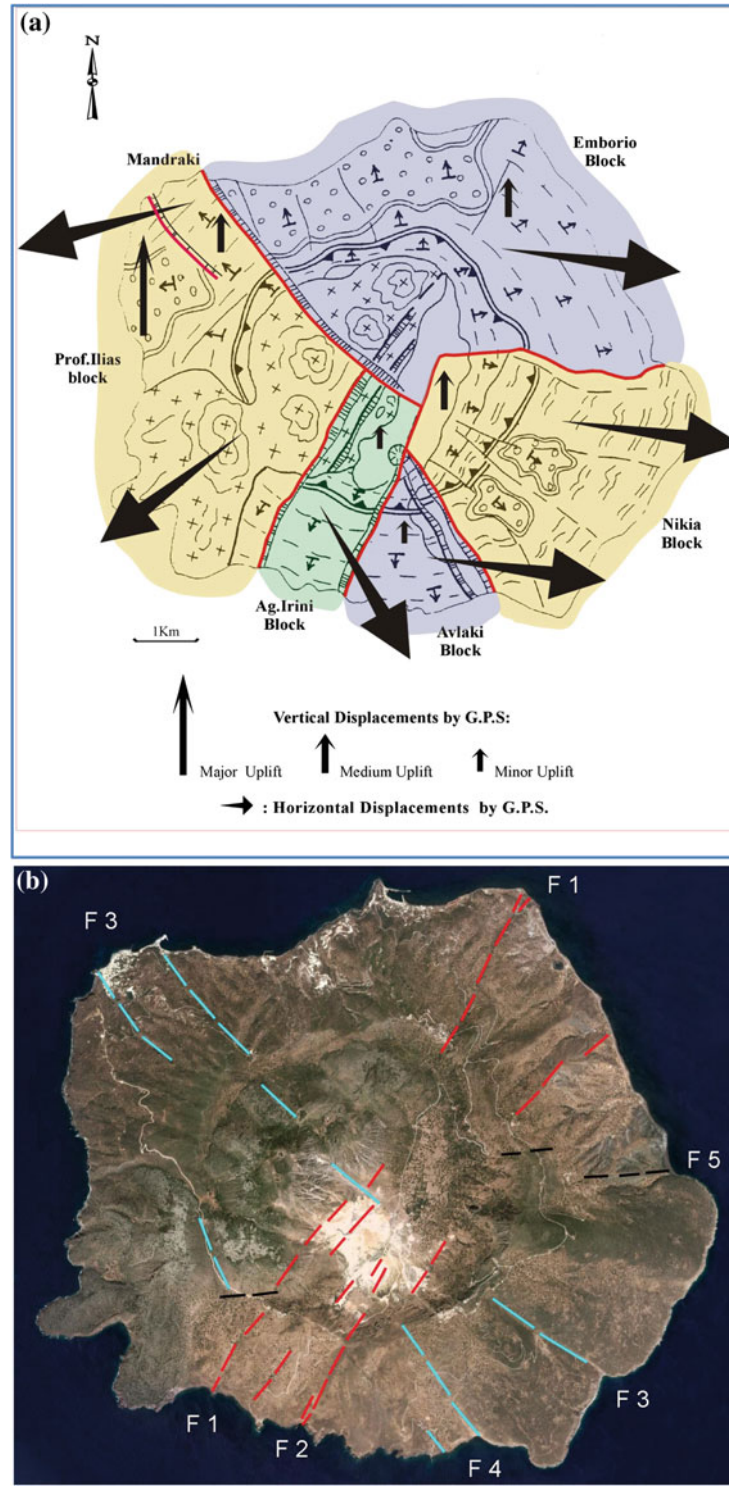

Fig. 3.3 **a** Simplified schematic geological map of Nisyros Island showing the major neotectonic blocks (Profitis Ilias block in *yellow*, Aghia Irini block in *green*, Avlaki block in *orange* and Emborio/Nikia block in *yellow*) resulting from the four major fault zones F1, F2, F3, F4, and F5 (Papanikolaou and Nomikou 2000); **b** F1–F5 fault zones on google earth image

major young plinian eruptive cycles, which produced the lower and upper pumice, as well as the large rhyolitic lava flows in the southeast of the island, the discussion focused on caldera formation during one or two collapse episodes (Papanikolaou et al. 1991; Limburg and Varekamp 1991; Vougioukalakis 1998). However, it is possible that the general shape and structure of the present-day caldera resulted from earlier depression, which is indicated by two large stratovolcano flank collapses, prior or simultaneously to the plinian eruptions. Volentik et al. (2005) could establish three older phreato-magmatic to sub-plinian eruptive phases during the early shield volcano cycles, which also emitted large volumes (lithostratigraphic units Nos. 4, 6, 11, Electronic Supplementary Material Appendix 3.3) of pumice fallout, pyroclastic flows, and surges. The existence of two lacustrine cycles could be interpreted as an early internal lake-stage with limited dimensions of probably few hundred meters only (Volentik et al. 2002) as an expression of a depression in north–eastern center of the island.

Despite alteration effects, no large hydrothermal deposits or strong hydrothermal alteration have been recognized as possible earlier indications of high-crustal level magma reservoirs accompanied with a post-eruptive caldera forming collapse.

3.2.2 The Fault Systems

Two major and three minor fault systems can be distinguished within the volcanic edifice of Nisyros Island (Figs. 3.1 and 3.3). The directions are in accordance with previous structural and geological investigations (Papanikolaou et al. 1991; Vougioukalakis 1993; Nomikou and Papanikolaou 2000, 2011):

- (F1, 2) N30E 1st order faults with local changes to NE directions
- (F3, 4) N30W 1st order faults with changes between N0° and N40°W
- (F5) E–W 2nd order faults
- (F6) N–S 2nd order faults
- (F7) WNW–ESE 2nd order faults (approx. 120°)

The NE–SW (F1, 2) 1st order fault system

F1 Fault Zone. It is located along the central part of the caldera comprising two or three parallel fault surfaces with a N30°E strike and a 70–80° dip to the SE. Its throw is more than 100 m and it separates the Profitis Ilias lavas and domes to the northwest from the caldera deposits to the southeast (Figs. 3.1 and 3.7a, b). Its morphological impact is very strong within the caldera and less outside of it. Towards the northeast it is not very prominent and there is no abrupt break of the caldera rim in the area of Emborios village.

F2 Fault Zone. This fault zone is parallel to F1 and runs along the southern caldera wall roughly 1.5 km southeast of F1 (Figs. 3.1 and 3.4). It strikes N30°E and dips 70–80° to the WNW forming a tectonic graben with the opposite facing F1 (Figs. 3.7a, b and 3.8). This graben structure comprises the remnant of the 160,000 years Kos caldera plain with lacustrine and alluvial deposits, known as Lakki plain. Its throw may be estimated to be about 100–120 m, on the basis of the offset of the lavas and pyroclastics of the lithostratigraphic units 17, 21, and 22 (Figs. 3.6, 3.7 and 3.8).

Horizontal displacements of the F1 fault system with dextral strike-slip motion and extension SE–NW have been interpreted from focal mechanisms of major earthquakes ($M > 5$) at shallow and intermediate crustal depths (Drakopoulos and Delibasis 1982).

The F1 system seems also to have played a major role during the emplacement of the post-caldera dacites (Fig. 3.7a, b). Their eruptive centers are aligned along an N30°–40°E striking fault plane. Since these magmas were derived from reservoirs at deep crustal levels, the F1 fault system must document a zone of weakness reaching the deepest crustal parts. Further evidence of such an interpretation can be taken from the spatial distribution of earthquake epi- and hypocenters.

The NW–SE (F3, 4) 1st order fault system

The major N30 W fault system have steep inclinations of 70°–80° at the surface changing

Fig. 3.4 Eastern part of the caldera rim with central and eastern hydrothermal craters with faults F1 and F2 (*red lines*). *Photo* V.J. Dietrich

Fig. 3.5 Fault breccia (autobrecciated dike) within the major NW–SE fault zone (F2) at the southeast rim of the caldera (road to monastery Ag. Stavros, Fig. 3.1); *Photo* V.J. Dietrich

the direction of dips depending on the geotechnical rock properties between NE and NW. These faults run perpendicular to the large Kos horst-graben system (Figs. 3.1, 3.9, 3.10 and 3.11). Characteristics of this fault system are extensional features and downfaulting up to 70 m. They extend from the northwestern parts of Tilos Island into Nisyros Island in the area of Avlaki, crosscut the entire island, run along the western part of Yali and merge into Kos Island at the "Paradise bubble beach".

The F3 fault zone is located in the northwestern part of Nisyros Island with a general trend to N30°W and dip 70–80° to the NE (Figs. 3.9 and 3.10). It juxtaposes different stratigraphic formations both within and outside the caldera. Inside the caldera it separates the main outcrops of the Profitis Ilias lava domes

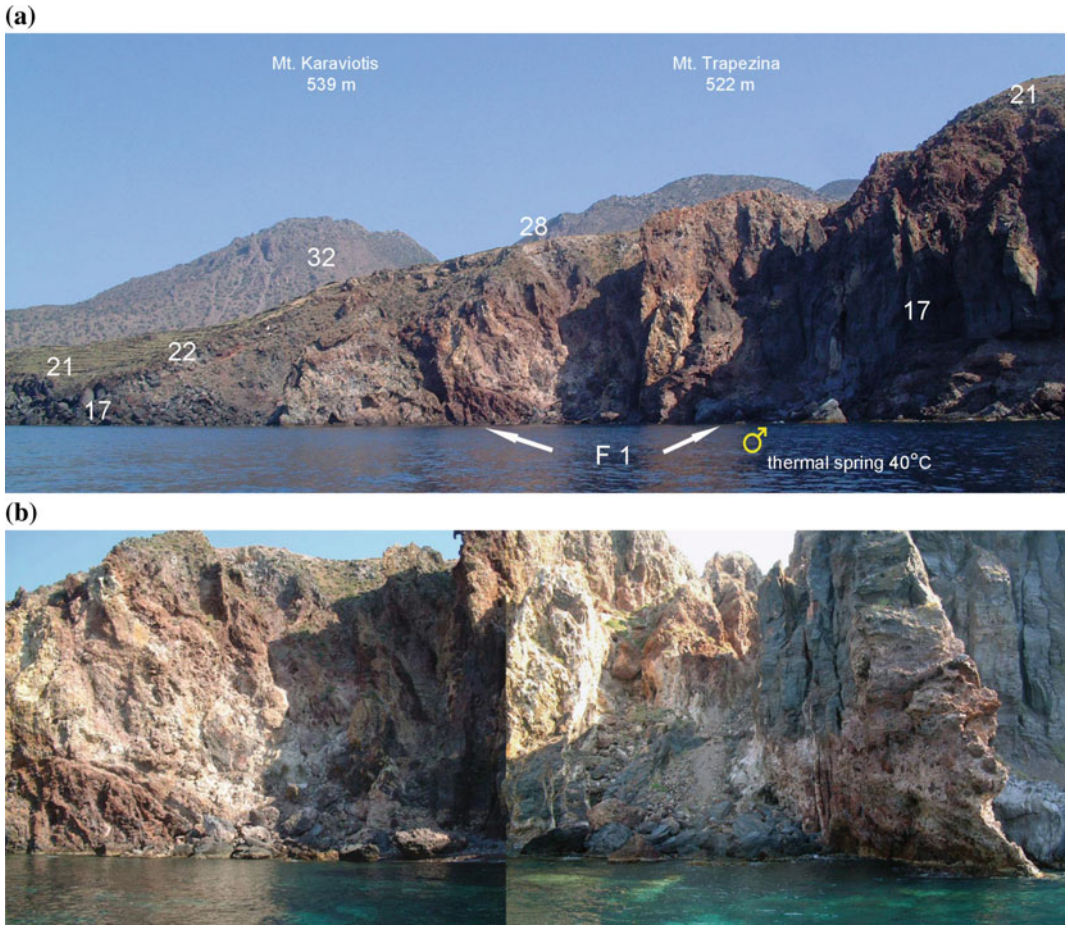

Fig. 3.6 **a** and **b** (close up) the major NE–SW (F2) fault system with chaotic hydrothermally altered fault breccia approx. 500 m east of Aghia Irini (Fig. 3.1). Numbers refer to lithostratigraphic units. *Photo* V.J. Dietrich

from the smaller domes to the northeast whereas outside the caldera it separates the outcrops of white pumice to the down faulted block in the northeast from the uplifted block in the southwest (where the pillow lavas No. 1 occur just above sea level). Its throw is more than 100 m.

The Mandraki fault runs parallel to the F3 fault zone at a distance of about 1 km to the southwest. The kinematic characteristics of the two faults are similar, with a general strike in the NNW–SSE direction and dip towards the ENE. The Mandraki fault is normal with a throw of about 100 m a.s.l indicated by the offset of the characteristic stratigraphic formations (Fig. 3.11a, b). The western block is topographically higher by 100 m and hosts the two important monuments of the island, which are the ancient castle of 4th century B.C. and the Panaghia Spiliani Monastery within the Byzantine/Venetian castle. The eastern block comprises the town of Mandraki with its westernmost buildings reaching the valley running along the Mandraki fault known as "Langhadi".

In continuation, a series of NW–SE parallel faults cut the Nisyros Island in the area of Avlaki and Aghia Irini (Figs. 3.1 and 3.6). Best evidence for downfaulting of the Aghia Irini block can be taken from the offset of the southern caldera rim. The fault system runs through the Stefanos Crater extending into the hydrothermal craters of Mikros Polyvotis and Megalos Polyvotis. One branch cuts through the domes of Profitis Ilias and Nifios into the northwestern crater rim and

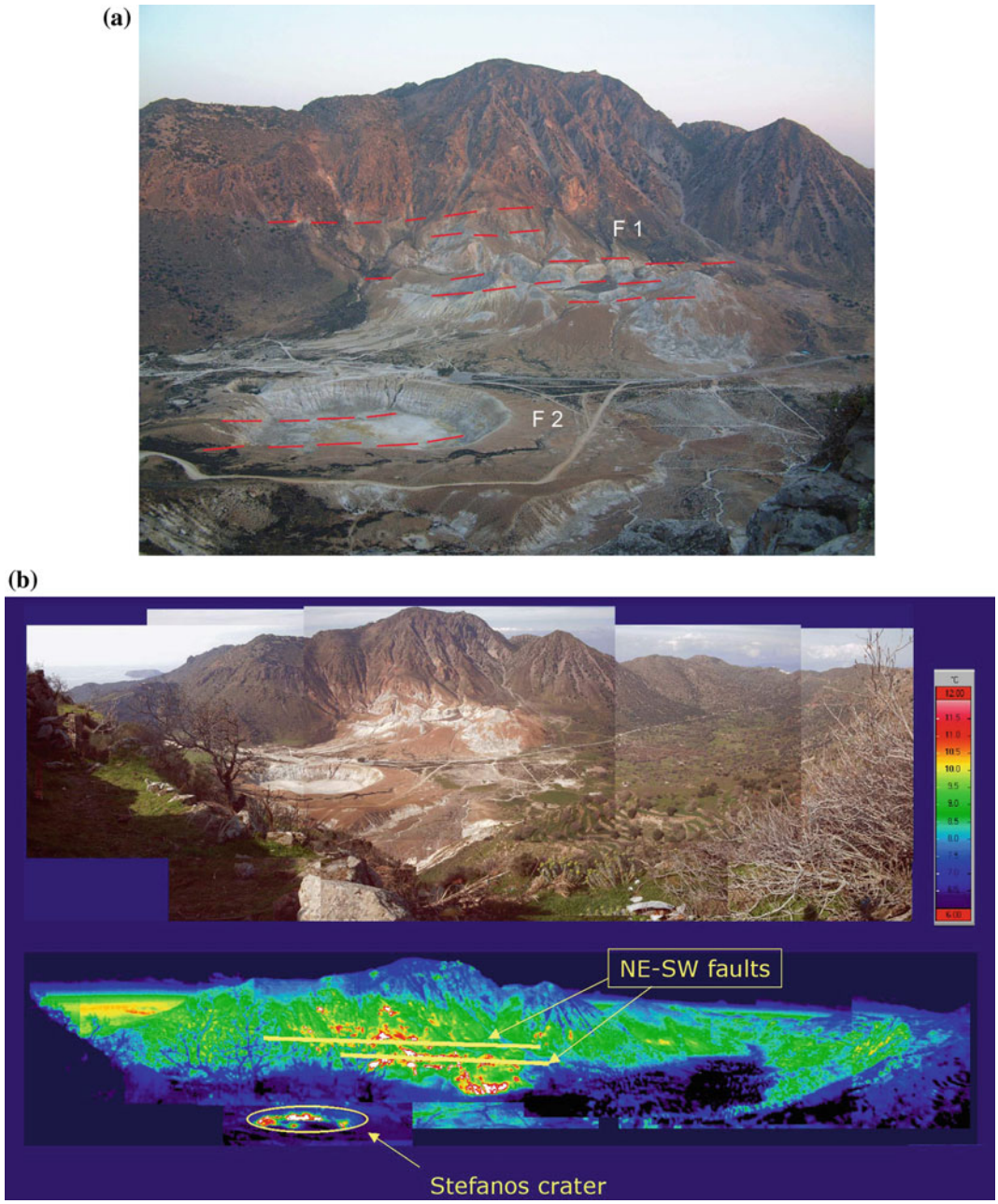

Fig. 3.7 **a** Recent fault systems inside the caldera linked to the hydrothermal explosion craters with faults F1 and F2. View from Nikia. **b** Thermal imaging of the hydrothermal crater field and the spatial distribution of the fractures and inferred faults F1 within the Profitis Ilias rhyodacitic domes. GEOWARN (2003). *Photo* V. J. Dietrich

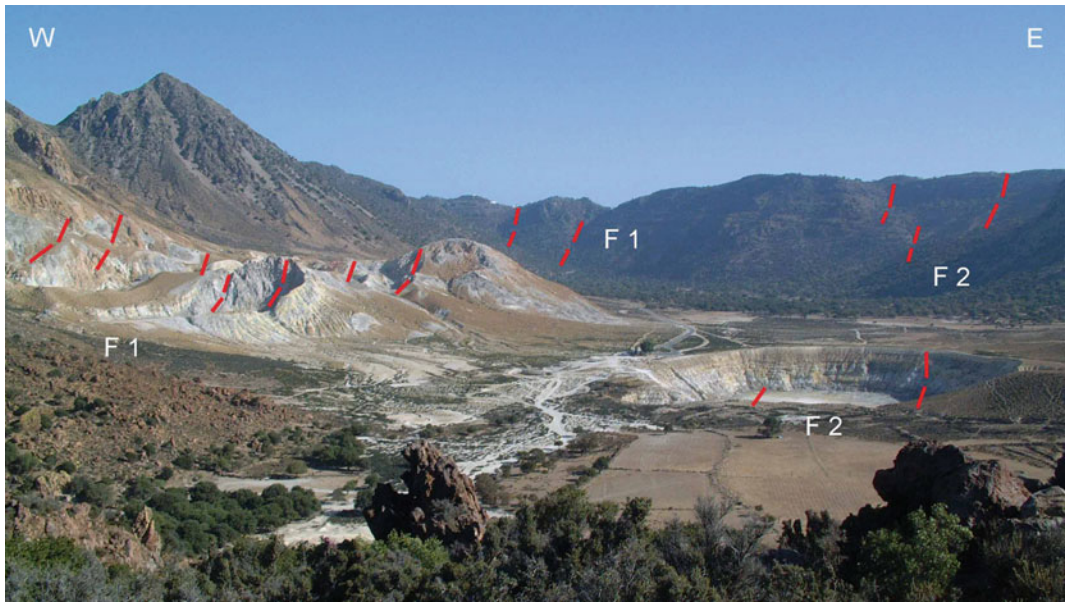

Fig. 3.8 Listric F1 and F2 fractures and faults in the northern part of the caldera rim and in the western and central hydrothermal craters. *Photo* V.J. Dietrich

splits into several minor faults west and east of the Monastery Evangelistra. There, the system forms a series of step-like downfaulted blocks between the Monastery Spiliani, the town of Mandraki and Loutra.

The F4 fault zone on Nisyros defines a tectonic graben, striking N20W, consisting of two conjugate faults with opposing dips. This fault zone is younger than the Nikia rhyolites (No. 30) and its throw is about 40–50 m. These fault zones of Nisyros Island produce a number of neotectonic blocks, each characterized by its relative uplift or subsidence (Fig. 3.3). The maximum uplift is observed in the western block/horst bounded by the F1 and F3 fault zones, which incorporates the maximum elevations of Profitis Ilias and surrounding summits. The maximum subsidence is observed in the southern block/graben of Aghia Irini, bounded by the F1 and F2 parallel fault zones.

All hydrothermal explosion craters are located in the intersections between the conjugate fault system F1, F2 and F4. At the northern and southern extensions of the F1 system, hot springs occur at sea level (Cape Katsuni and Thermiani in the north and Lefkos in the south). It is obvious from the bathymetric digital elevation model (BDEM) that these faults extend northeastward into the eastern Kos basin bordering the down-faulted slopes of Kos and the peninsula of Datça.

The rest of Nisyros Island constitutes the large neotectonic block of Emborio/Nikia, east of the F3 and F4 fault zones, with intermediate kinematic character since it has subsided with respect to the western block but has been uplifted with respect to the southern block. The Emborio area of the block is made of the stratovolcano stratigraphic formations, whereas the Nikia area is made of the Nikia rhyolite flows. A minor neotectonic block bounded by the F2 and F4 fault zones is observed in the southern part of Nisyros at the area of Avlaki with transitional character between the Aghia Irini and the Emborio/Nikia blocks.

The E–W (F5) 2nd order faults

The E–W oriented fault system seems to occur at present only at a local scale (Figs. 3.1 and 3.32a) and might represent a result of the deep reaching conjugate fault system F1 and F3. Surface expressions are visible along the north coast of Nisyros at the town of Mandraki, between the harbors Mandraki and Loutra, between Pali and

Fig. 3.9 F3 fault extension towards N and NW into Yali. *Photo* V.J. Dietrich

Fig. 3.10 Active NNW–SSE fault of Mandraki (*center*) extending into the central part of Yali island (*background*). *Photo* V.J. Dietrich

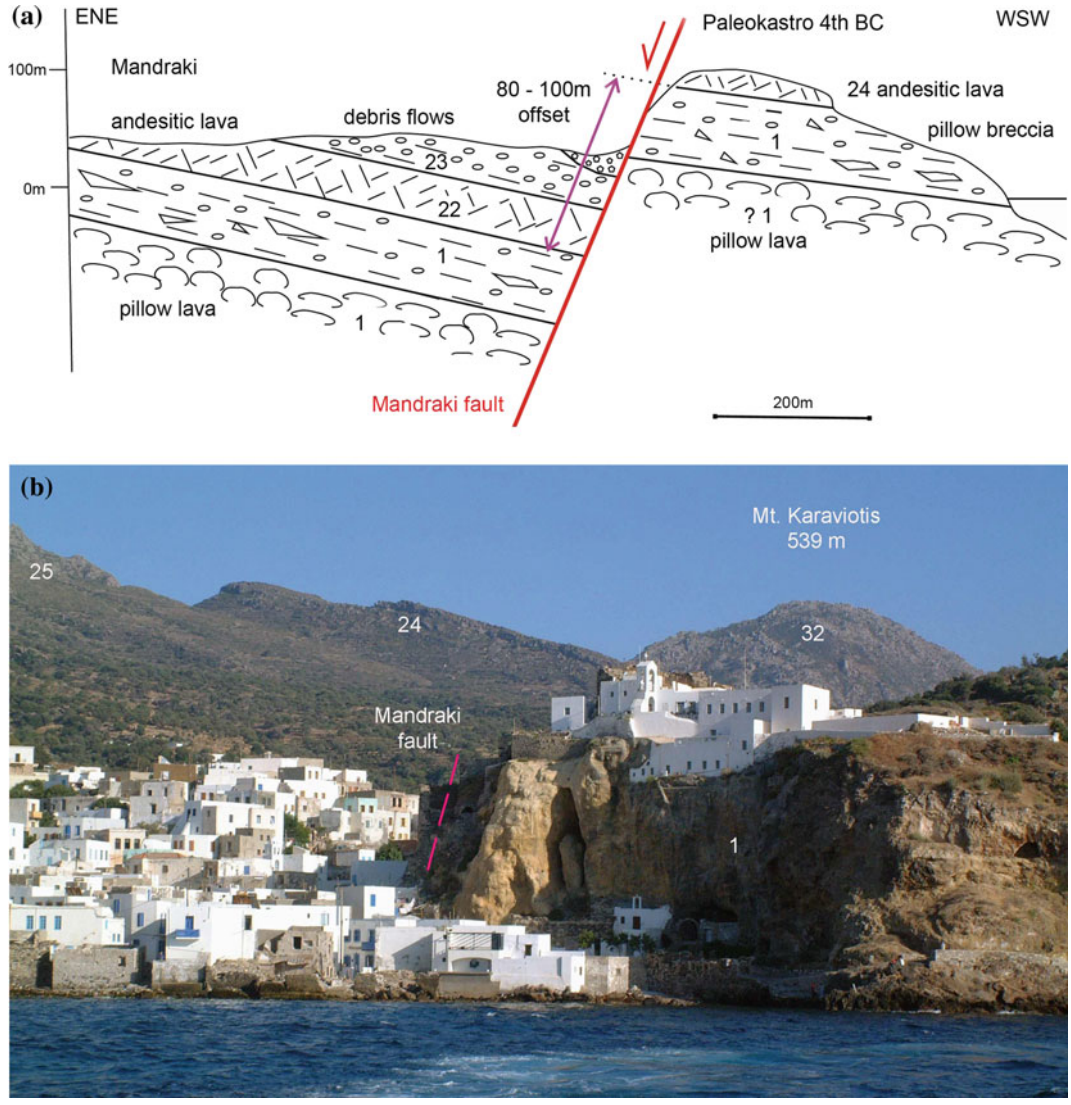

Fig. 3.11 **a** Vertical offset at the northwestern corner of Nisyros Island due to the NNW–SSE trending steep Mandraki fault F3 (Fig. 3.11b). Sketch *redrawn* after Papanikolaou and Nomikou (2011). **b** Monastery Panaghia Spiliani on the uplifted cliffs at the Northwest corner of Nisyros Island with the western end of Mandraki; view of the active Mandraki fault F3 from north between the western boundary of Mandraki. In the background lavas of LSU units Nos. 24 and 25 and Karaviotis dome Unit No. 32. *Photo* V.J. Dietrich

Faros, along the western Karaviotis lava flows bordering the Kateros cove and in the valley between the Monastery Panagia Kyra and the southern border of Pachia Ammos beach. The hot spring of Afionas at sea level might also be a result of this fault system.

The N–S (F6) 2nd order faults

A subordinate N–S fault system can be locally established in the volcanic edifice of Nisyros Island (Fig. 3.12): Along the northwest coast, between the rhyodacitic domes of Karaviotis and Trapezina and at Cape Akrotiri. According to the

Fig. 3.12 Cape Akrotiri with N–S fault. *Photo* V.J. Dietrich

bathymetric map (BDEM) the latter fault seems to extend into a small N–S graben between Yali and Strongyli (Fig. 2.6, Chap. 2). An equivalent system appears to also be present in the peninsula of Kefalos on Kos. Similar to the F4 system, the N–S might also be a result of the dominant conjugate F1 and F3 systems.

3.2.3 The Lakki Rupture 2001, 2002, and 2011

3.2.3.1 Annual Episodes of Rupturing

A large N–S trending fracture ("Lakki rupture") opened in the Lakki plain of the Caldera in early December 2001 (Figs. 3.13 and 3.14). Although this large rupture extended over a distance of 350 m and up to 5 m wide and up to 10 m (in few cases 20 m) deep, neither gas and thermal waters were recognized nor seismic signals were recorded. In December 2002, the fracture continued to extend southward for another 500 m showing smaller perpendicular offsets (Fig. 3.15). During a heavy rainstorm during November 12/13, 2011 another large rupture was formed (Figs. 3.16 and 3.17) intersecting the 2001/2002 rupture in the central part of the Lakki plain. The direction of the new rupture was NNW–SSE with approximately 320°, starting in the south as reactivation of the 2001 rupture and continuing for approximately 450 m towards NNW crossing the road. The northern and the southern parts of the old rupture were not affected.

3.2.3.2 Interpretation and Origin of Ruptures

The rupture is interpreted as surface stress release in the consolidated and cemented epiclastic and hydrothermal sediments of the caldera floor, due to progressive uplift and East–West extension of the central parts of the island since the seismic crisis 1996/1997 and a possible magma input at greater crustal depth (GEOWARN project 2003). No significant earthquake activity has been recorded during the formation of all ruptures.

In addition, subrosion by meteoric waters and their drainage from large cavities and tunnels several tens of meters beneath the Lakki plain

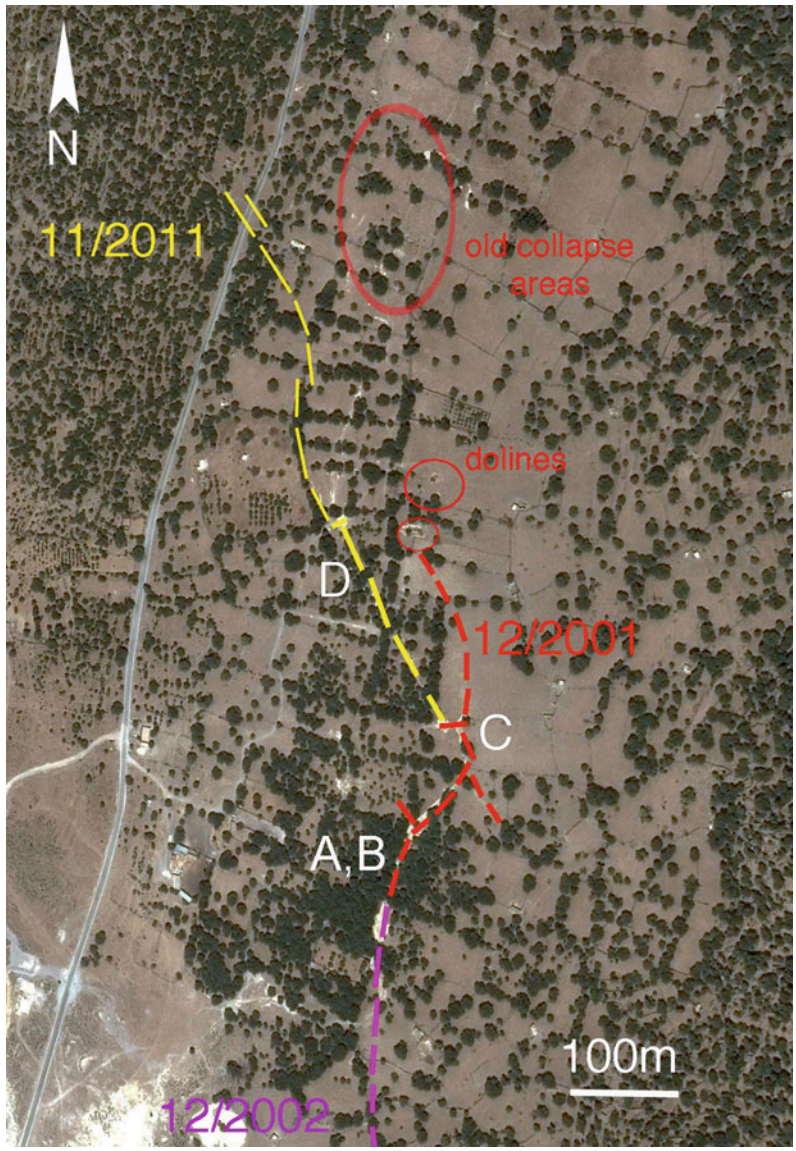

Fig. 3.13 Localization of the surficial, up to 20 m deep ruptures in the central part of the Lakki plain, which formed during three episodes during abnormally high precipitation in winter times: November 2001, December 2002, and November 2011. Image google earth

may have enhanced the stress release, leading to breakdown of ruptures and "doline type" holes (Fig. 3.13, location D). This interpretation is favored by the timing of the rupture formation after a long dry summer and fall during and shortly after the first large rainstorm in the beginning of wintertime (e.g. ruptures: 12/2001, 12/2002 and 11/2011).

The direction of the 11/2011 ruptures coincides with well-known NW–NNW trending fractures and faults cross cutting the island. Therefore, deeper zones of weakness in the island, expressed in form of fractures and faults enhance the weakening of the Lakki plain. However, the new rupture must be regarded as a simple surface phenomenon, since no heat, gases and hot waters have been recognized.

Fig. 3.14 Surficial, up to 10 m deep ruptures in the central part of the Lakki plain, which formed during the first episode in November 2001. Neither vertical nor strike-slip displacements are visible. Locality A in Fig. 3.13 view towards south; picture taken December 9, 2001. *Photo* A. Ganas

Fig. 3.15 Surficial, up to 20 m deep rupture in the central part of the Lakki plain, which was reactivated during the second episode during December 2002; The rupture partially widened and was filled with mud bushes and trees; locality B in Fig. 3.13 view towards south, picture taken March 13, 2003. *Photo* V.J. Dietrich

Fig. 3.16 Intersection of the 2001/2002 ruptures (*right* foreground with the rupture of the third episode, November 2011 (*left*, background). Indication of the intersecting process is demonstrated in the sharp surface edges. The rupture also partially widened and was filled with mud due to torrents caused by the strong rainstorms; The wall expose the upper several meters of argillitic to sandy layered sediments of the Lakki plain. Locality C in Fig. 3.13 view towards southwest; picture taken November 21, 2011. *Photo* V.J. Dietrich

Fig. 3.17 6–8 m deep and 8 m in diameter "doline-type" hole next to the rupture of November 2011. The filling was washed away through a drainage hole leading to a deeper system of subroded tunnels; locality D in Fig. 3.13; picture taken December 3, 2011. *Photo* V.J. Dietrich

According to all observations, the Lakki rupture does not indicate any volcanic phenomena or reactivation of magmatic activity at depth.

3.3 Detailed Lithostratigraphy of Nisyros Volcano

Volcanoes in oceanic and continental arc environments are built up mainly by eruptions of water-bearing ranging from basalts to rhyolites and eruptions of typically volatile-rich magmas. The life-time of a single volcanic edifice can vary from thousands to several millions of years depending on the geotectonic and geodynamic environment, thickness and constitution of the crust, and consequently on the emplacement and differentiation mechanism of the magmas through the crust to the surface (Hildreth 2007). The construction of these volcanoes occurs during eruptive episodes, that typically follow a cyclic pattern: An eruption generally starts with hydro-magmatic explosions, is followed by phreato-magmatic eruptions producing mostly fallout deposits and surges, then grades into magmatic explosive activity, feeding surges and pyroclastic flows, before, final emplacement of degassed lavas forming, domes and necks. These eruptive cycles are then followed by periods of dormancy, during which magma reservoirs get refilled. Hydrothermal activity can be important while the volcano is dormant, and the edifice typically undergoes intense erosion, sometimes catastrophically by flank collapse.

As the Nisyros volcanic history is based on the litho- and tephrostratigraphy of the edifice (mostly defined by the mapped lavas and pyroclastic rocks), it is best to describe it using these cycles of eruptive activity, separated by epiclastic deposits and the paleosols, which mark the periods of dormancy (Table 3.1). Depending on the state of development of these volcanoes, one can find initial, embryonal stages with short cycles of years to hundreds of years, and more evolved stages, composed of numerous equivalent short eruptive cycles merging into a major cycle with long temporal intervals.

The detailed lithostratigraphy of the Geological Map of the Island of Nisyros is given in the Electronic Supplementary Material Appendix of this chapter.

Table 3.1 Comprehensive presentation of the Nisyros lithostratigraphic units (LSU) 1–32, divided into eruptive cycles

LSU	Eruption mode	Thickness	Rocktype
	Post-Caldera eruptive cycle		
32	Lava domes, flows	Max. 600 m	Rhyodacite
	Epiclastic deposits	Max. 2 m	
	Caldera eruptive cycles and Caldera collapse		
31	FI-WS-FI-PbS-succ.	Outcrop 30 m	Rhyolite
30	Lava flows	Max. 150 m	Rhyolite
29	Epiclastic deposits	Max. 20 m	
28	F-FI-WS-FI-succ.	Outcrop 20 m	Rhyolite
27	Lava flow	Max. 10 m	Andesite
	Composite Stratovolcano cycles		
26	Dome collapse breccia	Outcrop 20–30 m	Dacite
25	Flows	Max. 150 m	Dacite
24	Flows	Max. 25 m	Bas. And.- Andesite
23	Epiclastic deposits	Max. 20 m	
22	Flows	Max. 10 m	Bas. And.- Andesite
21	F-PbS-PyFI-succ	Outcrop 15 m	Bas. And.- Andesite
20	Epiclastic deposits	Max. 20 m	

(continued)

Table 3.1 (continued)

LSU	Eruption mode	Thickness	Rocktype
19	F-S-F-3S-F-F-xS-F-succ.	Outcrop 50 m	Bas. And.to Dac.
19	F-PbS-FI-succ.	Outcrop 40 m	Dacite
18	Lava flow	? Max. 10 m	Dacite
17	Lava domes, flows	Max. 60 m	Rhyolite
16	S-FI-succession	Outcrop 30 m	Basaltic Andesite
15	Lava flow	Max. 40 m	Andesite
14	Lava flow	Max. 25 m	Dacite
13	Lava flow	Max. 40 m	Bas. And.- Andesite
12	Epiclastic deposits	Max. 2 m	
	Early shield Volcanic cycles		
11	F-FI-F-S-FI-succ.	Outcrop 35 m	Bas. And.- Andesite
10	Lava flows	Max. 70 m	Basaltic Andesite
9	Lacustrine deposits	Max. 5 m	
8	Lava flow	Max. 5 m	Basaltic Andesite
7	Lacustrine deposits	Max. 5 m	
6	S-F-FI-S-FI-succ.	Outcrop 60 m	Basaltic Andesite
5	Lava flows	Max. 40 m	Andesite
4	F-FI-S-F-succ.	Outcrop 30 m	Andesite
3	Lava flow	Max. 35 m	Basaltic Andesite
	Submarine Volcanic base		
1, 2	Pillow and lava flows	? Max. 50 m	Basaltic Andesite

3.4 The Eruptive History of Nisyros Volcano

3.4.1 Introduction

The island of Nisyros is a Quaternary composite stratovolcano located at the easternmost end of the Aegean volcanic arc, in the Dodecanese archipelago, south of Kos. The island is almost circular, with an average diameter of 8 km, covering an area of about 42 km^2. It lies above a basement of Mesozoic limestone (Geotermica Italiana 1983, 1984) and a thinned crust, with the Moho located at a depth of about 27 km (Makris and Stobbe 1984). The references of previous studies in volcanology, petrology, geochemistry of volcanic rocks, fumarolic gases and hydrothermal waters has been listed chronologically at the end of this chapter; geological maps have been published by Di Paola (1974), Papanikolaou et al. (1991), Vougioukalakis (1993, 1998, 2003), GEOWARN (2003), Volentik et al. (2005).

The volcanic edifice of Nisyros with a summit caldera of a 4 km average diameter is the result a large variety of explosive and effusive eruptions producing calc-alkaline pyroclastic deposits and lavas from basaltic andesitic, dacitic, rhyodacitic, and rhyolitic composition. According to previous studies, the volcanic history has been generally assigned to four major episodes: starting with shallow marine to subaerial basaltic to andesitic volcanism followed by moderate andesitic explosive and effusive activity, building up a first major strato-cone surrounded by several satellite eruption centers (scoria and tuff cones). The present morphology of the island is finally due to two major rhyolitic plinian explosive phases each accompanied with consecutive effusive voluminous lava flows and domes, which may have followed the caldera collapses.

3.4.2 Early Shield Volcano Cycles of Nisyros

3.4.2.1 Submarine Volcanic Base

Nisyros is entirely volcanic: metamorphic or sedimentary rocks have been mapped anywhere on the island. Geothermal drilling from the lowest part of the caldera in the Lakki plain (Well NIS 1 in the southeastern side at 110 m altitude asl and NIS 2 at the eastern foot of the young rhyodacitic Lofos dome at the western side at 145 m a.s.l) reached Mesozoic limestones at a depth of approximate 650 m depth bsl. The 750 m caldera filling consist of unconsolidated talus and alluvial deposits in the upper 150 m and poorly-documented tuffs, pyroclastic flows intercalated with basaltic to andesitic flows and epiclastic breccias in the last 600 m (Geotermica Italiana 1983, 1984). The evolution of the volcanic history of Nisyros Island described in this paper is solely based on the outcropping litho- and tephrostratigraphic successions.

The oldest occurrence of volcanic activity is represented by a shallow submarine to subaerial formation of hyaloclastites (LSU No. 1), pillow breccia, and pillow lava of up to 50 m thickness in the north–western corner of the island in the cliffs of Monastery Panagia Spiliani at Mandraki and in the western coastal part between Hochlaki beach (Fig. 3.18) and Cape Kanoni (Fig. 3.20). The hyaloclastics and loosely packed pillows and pillow breccia appear to be the front of subaerial basaltic andesite lava flows, which covers the brecciated units. A few dikes cut the whole formation; internal tilting and faulting is present. Extrusions from submarine fissures seem to be unlikely, since no typical close-packed pillow lava is present. To produce such high amounts of pillow breccia and hyaloclastic, palagonized material, an explosive origin from shallow submarine a subaerial vents, similar to processes forming peperites (Skilling et al. 2002; de Goer de Herve 2008) are envisaged. Such a process might be supported by intercalated lava lenses of variable thickness (up to 10 m) within the pillow-hyaloclastic sequence, partly mixed with intensively hydrothermally altered tuffs and tuffites (LSU No. 2, Fig. 3.20). The outcrops occur at Cape Kanoni and along its southern coastal strip. Since they are aligned to NE–SW (approx. 30°) tending faults, they could also be interpreted as channel fills.

Similar volcanic and volcanoclastic sequences have not been clearly linked to specific units in

Fig. 3.18 Basaltic andesite "pillow-hyaloclastite" formation (unit No. 1, Figs. 3.11b and 3.19), the lowest outcropping volcanic rocks of Nisyros volcano. The whole unit has an inclination of 20°–30° towards W–NW. The horizontal hatched *lines* represent erosional levels of different stages of uplift. *Photo* V.J. Dietrich

Fig. 3.19 The majority of the basaltic andesite clasts and pillow fragments, with an average diameter of 10–15 cm are embedded in a consolidated *yellow* to *orange* palagonitic cement. Isolated irregular pillows have variable diameters from 0.5 to ca. 8 m and occur mainly at the base of the unit. *Photo* V.J. Dietrich

Fig. 3.20 West coast at Cape Kanoni LSU units Nos. 1, 2, 20–24, and 28. From sea level to top: Talus, No. 1 (hyaloclastite formation; lower part "pillow breccia" overlain by tuffaceous deposits), No. 2 (tuffaceous deposits), 21 (pyroclastic flow), No. 22 (Basaltic andesite lava flow), No. 23 (Paleokastro epiclastic deposits), No. 24 (Basaltic andesite lava flow with thick red scoria sole and top and columnar jointing, unit 28 (lower pumice). *Photo* V.J. Dietrich

the geothermal wells. However, between −480 and −540 m b.s.l depth, breccias and a fine tuff/tuffite occurs on top a several ten meter thick "blocky tuff in a palagonitic matrix" (−540 to −585 m b.s.l). These units are suspiciously similar in two ways, and either they represent equivalents of the KIU-formation, the "Kos acoustically incoherent unit within the sedimentary cover in the west- and east Kos basins (Fig. 2.10) as part of the 161 ka Kos-Plateau-Tuff (KPT) eruption cycle (Stadlbauer 1988; Smith et al. 1996; Allen 2001; Bachmann 2010), or local eruptive equivalents of the early volcanic cycles of Nisyros Island.

A paleogeographic reconstruction of the volcanic environment is difficult to achieve because of the lack precise data from the geothermal drill holes in the caldera. However, the thickness and extension of the "hyaloclastite formation" units Nos. 1 and 2 allows to establish a volcanic edifice similar to a subaerial shield volcanic structure, most probably with vents aligned a NE–SE trending fracture zone from were the lavas were emitted. In addition, a tilting towards NW is obvious due to unconformities in the hyaloclastite formation, e.g. within the uplifted cliffs of the M. Panaghia Spiliani.

The autobrecciation of the atypical pillow lava and pillow breccias without typical glassy rims und textural changes between outer and inner parts of the pseudo-pillow fragments leads to an interpretation either of water intrusion into the vents at very shallow aquatic levels or lava into muddy tuffaceous sediments, and thus instant brecciation. Similar brecciation processes have been described for the formation of peperites within small volcanic maar-lakes (for review see Skilling et al. 2002).

Up to now, no marine fossils have been found within the yellowish palagonitic matrix.

3.4.2.2 Early Nisyros Shield Volcano Cycles

The following volcanic activity comprises three major cycles, producing pyroclastics and lavas with basaltic andesite composition, but slightly different in their eruption characteristics. The exposures of these cycles are limited to the eastern parts of the inner caldera cliffs between Kato Lakki and Chonia and represent mainly proximal facies deposits (Figs. 3.21 and 3.22). Time intervals between these cycles must have been short, as erosional contacts or signs of paleosol are missing.

At the north–eastern lower part of the inner caldera above the Lakki plain, a subaerial lava flow up to 35 m thick and covering a distance of 1.2 km, records a first major subaerial eruption (unit No. 3). The lower part appears in several places strongly tectonised, which likely indicate recent faulting, such as break down and collapse of

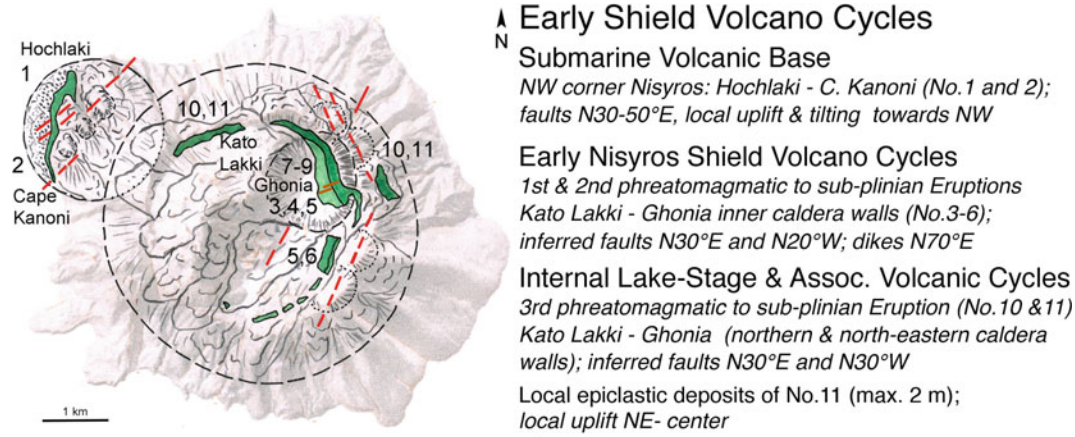

Fig. 3.21 Evolution of Nisyros volcano during the "Early Volcanic Cycles": Submarine volcanic base, early shield volcano cycles, internal lake-stage volcanic cycles

Fig. 3.22 View from S towards northeastern inner caldera walls with the lithostratigraphic units 3–15; *P* Parletia rhyolitic neck. *Photo* V.J. Dietrich

the caldera. It is possible that this cycle started with a major strombolian eruption, producing surges and pyroclastic flows, although such deposits are not preserved due to the coverage with talus and alluvial filling of the caldera. Papanikolaou et al. (1991) have correlated this lava flow with the stratigraphically lowermost basaltic andesite pillow and hyaloclastite sequence at the north–western corner of the island.

A second eruptive cycle (Fig. 3.23), producing ca. 35 m of pyroclastic deposits during a violent explosive phase (unit No. 4) seems to have started within a short time interval after the effusion of the underlying lava. The eruption started with a typical sub-plinian phase followed by a sequence of fine-grained pyroclastic flows and surges and terminated again with sub-plinian eruptions. The subsequent effusion produced an up to 40 m thick lava flow with a basaltic andesite composition (unit No. 5).

The explosive phase of the third cycle (unit No. 6) started with the deposition of coarse-grained planar-bedded surges indicating a high water/magma interaction ratio. After a short period of fallout, two thick pyroclastic flows, disrupted by two coarse-grained surges, planar bedded and with sandy-waves, were deposited.

The geometrical distribution and chemical similarity of the volcanic edifice produced during these three eruptive cycles during one consecutive period of time leads to the assumption of the generation of a subaerial shield volcano with a maximum diameter of several kilometers and a height of a few hundred meters. The large volume of erupted material during the third cycle, producing up to 60 m of pyroclastic deposits, the high lithic content of large fragments with an average size of 25 cm in the upper pyroclastic flow and the dip of the underlying lavas with respect to the present day caldera depression, support a collapse of the early shield volcano, leaving a small caldera behind (Volentik et al. 2002).

The geometric distribution and thickness of the lava and pyroclastics allow to a certain extent a reconstruction of the early volcanic edifice. A subaerial volcanic shield with a center more or less in respect to the present day caldera seems to be the most feasible interpretation. The lavas show slight inclinations and reduction of thickness outward. Indication of the position of the original vents can only be taken from the direction of a few dikes in the north–eastern caldera wall, which trend N 70°E. We assume that at this early volcanic stage the general structural trends

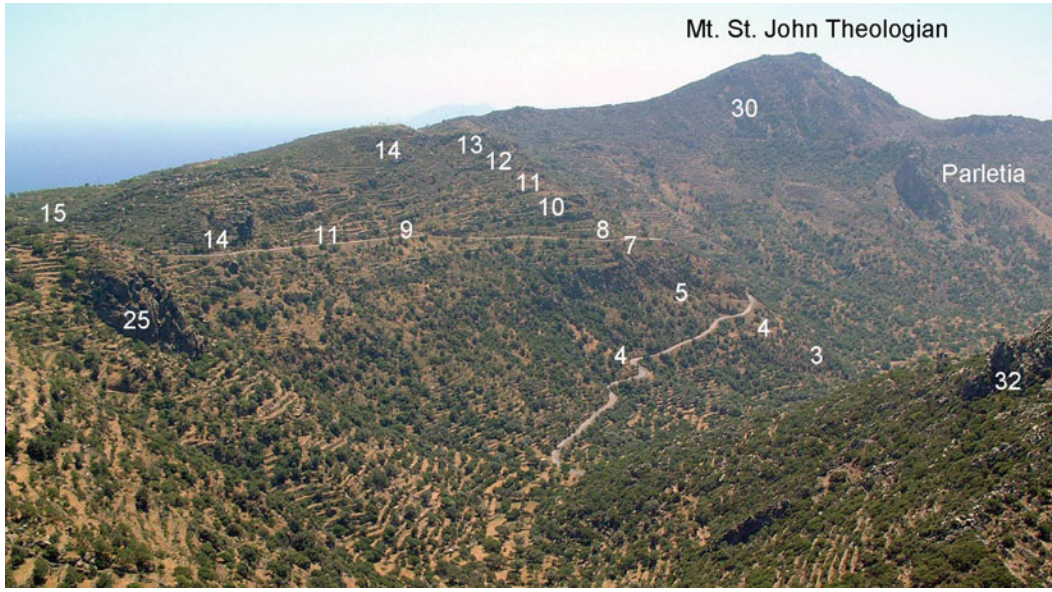

Fig. 3.23 View towards SE of the north–eastern inner caldera walls with the main road to the caldera floor (Lakki plain); in the background Mt. St. John Theologian 589 m and Parletia neck (rhyolite). Successions of the caldera walls from *bottom* to *top*: Lithostratigraphic units Nos. 3–15. The highest mountain of the eastern caldera rim St. John Theologian 589 m. *Photo* V.J. Dietrich

and tectonics of the regional volcanic field controlled the emplacement of magmas from the upper mantle through the crust to the surface. The conjugate faults, N30°E and N20°W seem to have played the most important role.

3.4.2.3 Internal Lake-Stage and Associated Volcanic Cycles

In the north–eastern part of the internal caldera cliffs between Kato Lakkì— Ghonia and on top of the three pyroclastic and lava cycles described above, two volcanoclastic, lacustrine sedimentary successions (LSU Nos. 7, 9) are found (Figs. 3.24 and 3.25). They are continuous over a distance of five hundred meters, divided by a few meters thick subaerial basaltic andesite lava (unit No. 8), indicating the presence of an "internal lake" within a period of minor volcanic activity. The fact that the lower contact of the intermediate lava flow is very sharp and without any sign of scoria or development of pillowed breccia shows that the early lake must have been shallow.

The varved beds of the two intra-caldera lakes and associated volcanic cycles indicate sedimentation of volcanic ashes and fine-grained lapilli mixed with sandy layers within an aqueous system (details in Electronic Supplementary Material Appendix 3.3; Volentik et al. 2002). Characteristic maar-type phreatomagmatic sedimentary structures have not been observed. These sediments seem to be limited in their lateral extension to the north–eastern segment of the caldera, since they are absent in other similar stratigraphic positions inside the caldera wall. Surge deposits are few in the lowest part of the section, but become abundant at the upper part. The lifetime of the two lacustrine cycles could not have exceeded several hundred to a thousand years due to the restricted thickness of the varved successions.

The lake stadium was terminated by an effusive cycle (unit No. 10), which produced several basalt-andesitic flows with scoriaceous base and top, building up 70 m of the northern and north–eastern caldera walls (Fig. 3.26), forming the cliffs below the village of Emborio, and cover the eastern slopes towards Kremastos. Since these units are also exposed in the southern inner caldera cliffs, although with reduced thickness, they

Fig. 3.24 Lapilli tuffs, varved tuffaceous sandstones (unit No. 7) with impact sag. The main part of the varved lacustrine beds consists of fine-grained purple and whitish sandstones, partly with cross-bedding. *Photo* V.J. Dietrich

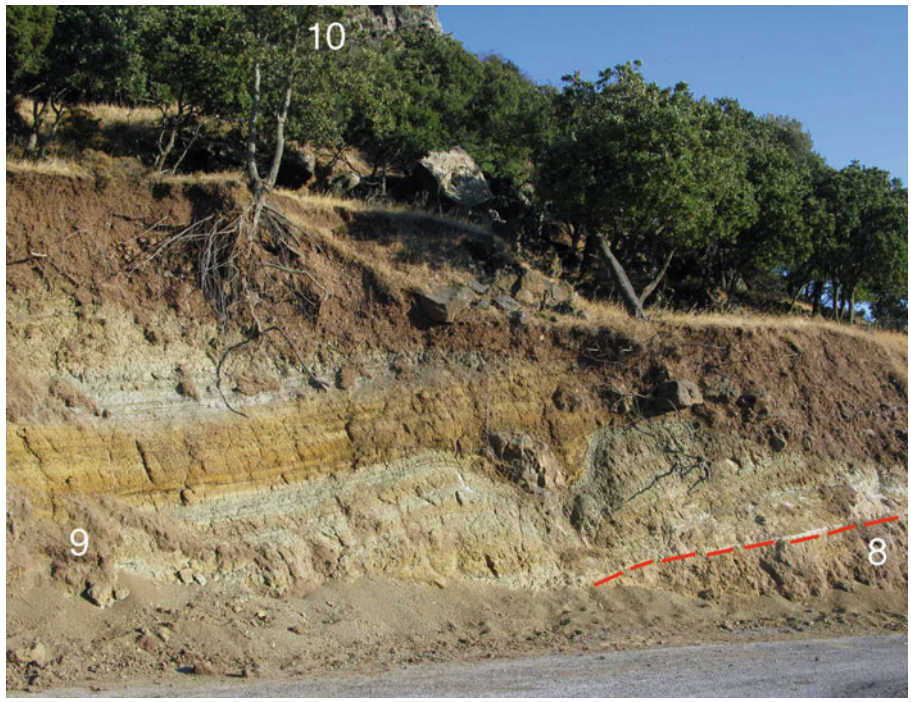

Fig. 3.25 Lower part of the second (*younger*) lacustrine succession of alternating siltstones (*purple*) and epiclastic sandstones (No. 9) with sharp contact to underlying reworked andesitic scoria of No. 8; large andesitic impact sag in the centre of picture; outcrop along the caldera road. *Photo* V.J. Dietrich

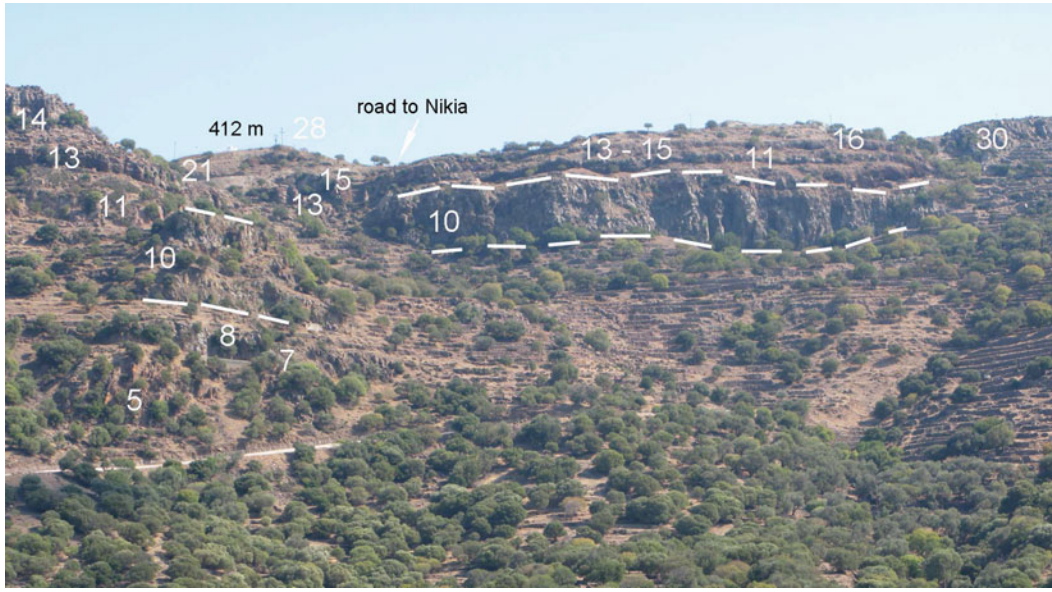

Fig. 3.26 Sequence of lavas and pyroclastic LSU Nos. 5–16 in the north–eastern inner caldera walls. *Photo* V. J. Dietrich

likely represent the filling of the early caldera with a diameter similar but smaller than the present day one. The neck west of the Kato Lakki plain can be seen as one of the eruptive centers.

Soon after the end of this effusive episode, a major explosive cycle started from a vent most probably located within the northern part of the caldera, covering the northern and eastern slopes of the island with 35 m of pyroclastic deposits (unit No. 11). This cycle started with a high explosive sub-plinian activity erupting a characteristic red pumice fall-out and intermittent fine-grained surges followed by strong pyroclastic flows including large blocs of lithics and pumice at their base.

The cycle terminated with a minor surge and fallout. The growth of a stratovolcano on top of the relicts of the early caldera may have been the result of the last strong explosive cycle. Minor epiclastic deposits (unit No. 12), which contain reworked material of the underlying pyroclastic succession, indicate both a time gap of volcanic activity permitting erosion and tectonic movements, e.g. local uplift between the NE corner and central part of the island and could be interpreted as bulging effect of a magma emplacement in the upper crust.

3.4.3 Composite Stratovolcano Cycles

3.4.3.1 Transition from Shield Volcano to Stratovolcano (Northern and Eastern Eruptive Centers)

After an unknown time gap, several short volcanic cycles contributed to the growth of a stratovolcano, erupting more evolved magmas from a central vent and from peripheral volcanic vents more or less aligned along the major regional fault systems (N30–50°E & N30°W; dike N20°W). This volcanic period can be limited between the early epiclastic deposits (unit No. 12) and the wide spread epiclastites and conglomerates of Paleokastro (unit No. 23) and with a sequence of three dominant lava flows (LSU Nos. 13–15) derived from northern and eastern central eruptive centers (Fig. 3.27). These flows form the upper parts of the caldera walls in the northern, northeastern and eastern segments and cover the north–western slopes down from Monastery Evangelistra and the eastern slopes between the areas of Linevrochia and Kremasto.

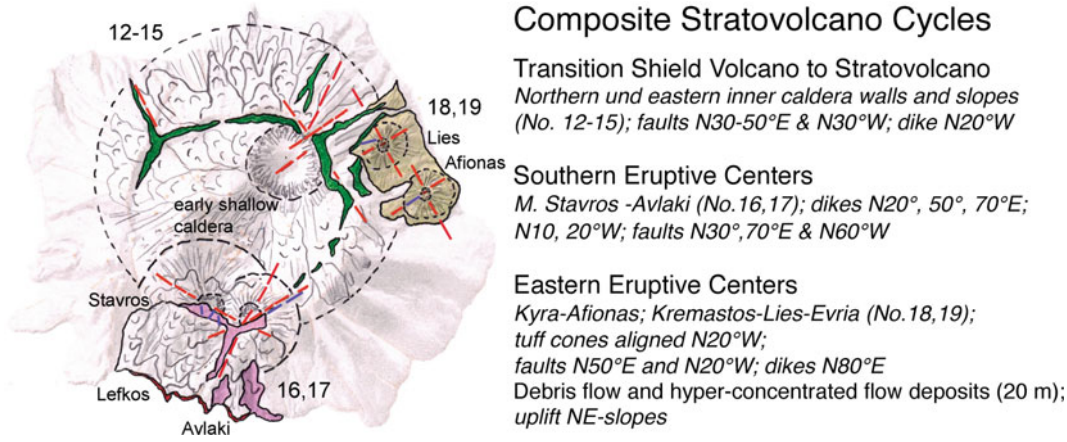

Fig. 3.27 The transition from shield volcano to stratovolcano and the clear distinction between two eruptive areas, the southern and eastern eruptive centers

Fig. 3.28 Neck (up to 40 m) within the andesitic lava flow, unit No. 13, exposed towards north outside the caldera call east of Emborios. *Photo* V.J. Dietrich

During this new cycle, more differentiated (andesite and dacite) magmas reached the surface. The first, 40 m thick andesitic lava flow (unit No. 13, Fig. 3.28) was emitted from a main central vent, since it appeared all around the upper caldera walls with the exception in the southwest, where the young Profitis Ilias rhyodacitic lava flows probably cover it. An andesitic neck and a small scoria cone in the upper eastern slopes close to the present day caldera rim represent two additional satellite eruptive centers.

A 25 m thick dacitic lava flow (unit No. 14), which covered the andesitic lava without any observable time break, erupted most probably from the same central vent. It is present from the village of Emborio throughout the northern and eastern segments of the upper caldera cliffs and extends towards south in the cliffs below the village of Nikia. This unit contains up to 30% of andesitic inclusions with both reddish and grey colors. The grey enclaves appear quenched, and likely indicate the reinjection of andesitic magma into a dacitic reservoir. The red oxidized andesitic inclusion, in contrast, are interpreted as older lithic material incorporated into the dacitic magma during the emplacement.

The final, 40 m thick andesitic lava flow (unit No. 15) forms the top of the "lava trilogy cycle" with a thick base of red scoria. It covers mainly the upper northern segment of the caldera and parts of the northeastern slopes of the island.

3.4.3.2 Southern Eruptive Centers (Monastery Stavros—Avlaki)

The following volcanic sequences can mainly be assigned to remnant eruption centers, which are exposed in the southern segment of the caldera walls below the Monastery of Stavros and cover the southern slopes (between the coves of Lefkos in the southwest and Aghios Nikolakis, Avlaki) with pyroclastic flows and lava (Figs. 3.27 and 3.29). They are assigned to one eruptive cycle slightly younger than the previous "trilogy cycle". The beginning of this cycle starts with a 30 m thick basaltic andesite pyroclastic succession of several small base surges of grey lapilli followed by pyroclastic flows, rich in andesitic lithics (unit No. 16). The strong hydrothermal alteration, within this unit (including the lithics) requires the existence of a larger magma reservoir at higher crustal depth and heat supply to a hydrothermal system.

Fig. 3.29 View towards southwest from Nikia (Monastery Stavros and Pachia island in the background). Note the depression of the western segment controlled by two major fault zones. On the *left* the rhyolitic lava flows and neck of Tsimi hill with the Mylos tower (old mill). *Photo* V.J. Dietrich

Fig. 3.30 Rhyolitic lava, unit No. 17 with internal flow folding and original surface. South coast, west of Avlaki *Photo* V.J. Dietrich

The cycle ends with the effusion of voluminous, up to 40 m black, massive, partly glassy, and perlitic rhyolitic lava flows (unit No. 17, Fig. 3.30). The Tsimi neck west of the Village of Nikia at the southern caldera rim marks one eruptive center of the blocky lava. Other vents are probably covered by the young rhyodacitic domes and lavas in the southwestern segment of the caldera.

The different trends of the dikes N20°, 50°, 70°E; N10, 20°W, as well as the measurable faults N30°, 70°E and N60°W indicate a complex extensional system along which the magmas were emplaced.

3.4.3.3 Eastern Eruptive Centers (Tuffs Cones of Kyra—Afionas; Kremastos—Lies—Evria)

The eastern flanks of the island comprise several similar eruptive cycles represented by successions of surges, pyroclasic flows and fallout which may have been derived from at least two major eruptive centers, the hills of Afionas and Lies, both remnants of large tuff cones (Fig. 3.27). Most of the unconsolidated tuffs have been eroded and washed down into the sea during rainstorms and mudflows, causing small frontal deltas and submarine channels close to the shore. In addition, the entire area of the eastern slopes resembles a large down-faulted block between major regional fault systems (Fig. 3.29 and structural Sect. 3.2). The two cones tuff cones seem to have been aligned along N20°W faults intersecting N50°E faults. A dike strikes N80°E.

Their ages cannot be precisely determined by lithostratigraphy. On the eastern slopes, these successions overlay older andesitic and dacitic lavas derived from the eastern caldera walls (the "trilogy cycle", units Nos. 13–15), while, to the South, everything is covered by the thick younger rhyolitic lavas flowing down from the south–eastern caldera rim. Only one light grey dacitic flow (unit No. 18), occurring at sea level along the shore at the base of Afionas tuff cone over a distance of 300 m between the beaches of Lies and Pachia Ammos, could be correlated with the first dacitic flow of the island (unit No. 14). However, this flow has slightly different

petrographic characteristics (e.g. the lack of abundant andesitic inclusions). Over a distance of 150 m, the surface of this grey dacite contains up to 1.6 m deep pockets filled with a strange brecciated fine-grained whitish rhyolitic flow with irregular enclaves of "andesitic schlieren" and mafic cumulates. In places, the yellowish color indicates the formation of a paleosol.

The andesitic to dacitic pyroclastic successions of the *Afionas tuff cone* (No. 19, Figs. 3.31 and 3.32), with a maximum thickness of 80 m, comprises at least three major explosive cycles from the same vent, separated by erosional contacts and thin paleosols. The deposits consist of light gray surges, proximal strombolian fallout and minor pyroclastic flows. The fallout contains lithics of andesite lava fragments and cumulates, in addition to limestones and contact metamorphic marbles and calc-silicate skarns. The fresh lithic andesitic fragments suggest that a recharge of andesitic magma into a dominantly dacitic reservoir occurred shortly prior to the eruption. A detailed stratigraphic description is given in the Electronic Supplementary Material Appendix 3.3.

Fig. 3.31 Tuff cone of Afionas (LSU Nos. 18, 19). The white-hatched line designates the general division of the Afionas tuff cone (Rehren 1988). *Photo* V.J. Dietrich

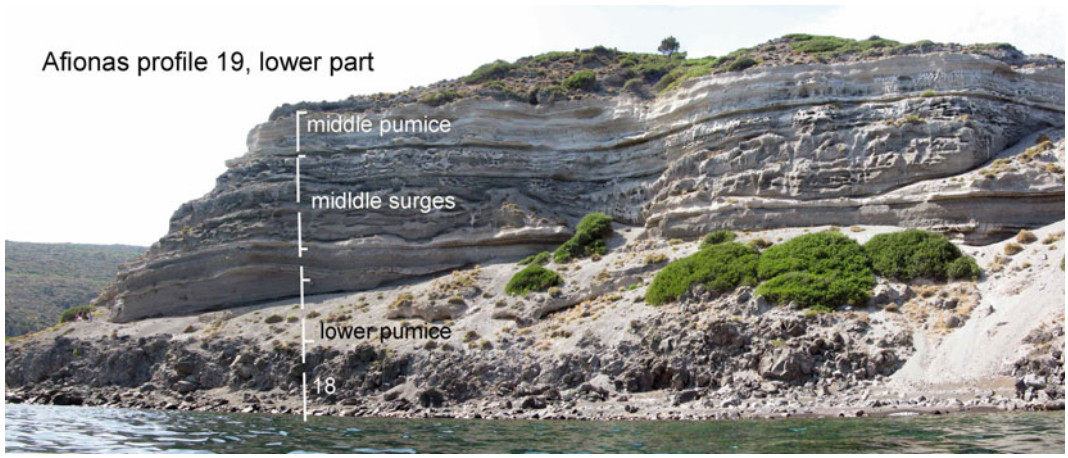

Fig. 3.32 Tuff cone of Afionas. At sea level dacite lava flow (unit No. 18), unconformatly overlain by a fall-surge-fall-surge-fall succession of bimodal composition, andesite and dacite. The *white* characteristic layer is made up surge deposits with planar-bedded and sandwave structures. *Photo* V.J. Dietrich

3.4.3.4 The Composite Stratovolcano (Mandraki—Pali—Kremares)

Lavas and pyroclastic deposits from the growing composite Stratovolcano occur throughout the island, typically in lateral cones, and are associated only in parts with the underlying sequences. They include remnants of cinder, spatter and scoria cones. This random distribution indicates that smaller eruption centers as lateral vents from radial feeder dikes could were formed around a central growing stratovolcano within the limits of the early caldera. The deposits from the peripheral vents contributed to the growth of the entire island.

The locations of the vents seem to be controlled at the by main fault pattern, N30°E, N70°E, as well as N30°W, N60°W, and E–W (Fig. 3.33).

The duration of this volcanic activity period can only be estimated by relative litho-stratigraphy and by the appearance of erosional features and paleosols. Since the latter time markers are missing, a rather short time period of several hundred to a few thousand years is envisaged. This assumption is compatible with the occurrence of the basal debris flows on the eastern flanks and in channels (unit No. 20), which require uplift, leading to massive (up to 20 m thick) debris flow deposits of reworked underlying pyroclastics (unit No. 19), channeled within deep valleys in the eastern flanks.

In addition, remnants of basaltic andesite cinder/scoria cones of strombolian activity have been recognized all over the island (unit No. 21, e.g., East of Ag. Marina and east of Koftaka (western flanks), south and north of M. Evangelistra, west of Akimaronas at the caldera rim, at Linevrochia and Kremastos on the eastern flanks (Fig. 3.34), at M. Stavros and at Tsimi on the southern caldera rim, and north of Avlaki in the southern flank (Fig. 3.35).

These small individual eruptive cycles have been combined into one up to 20 m thick pyroclastic unit of black lapilli, red and black scoria fallout deposits, spatter cone facies with agglutinated fragments of fresh lava and of planar-bedded surges (Fig. 3.36). In few cases, proximal thick and unsorted basal fallout deposits indicate violent strombolian eruptions as early phases. Often the scoria cone deposits contain abundant lithic components, such as fresh andesitic lava, anorthositic and amphibole-pyroxene-rich cumulates, limestones, contact metamorphic marbles and skarns. Several small basaltic andesite lava flows (unit No. 22) with individual thickness up to 10 m are closely associated with pyroclastic deposits described above and have originated as effusive part from the same spatter and scoria cones.

The stratovolcano period probably ended with a major summit collapse since up to 20 m thick debris flows with hyper-concentrated flow

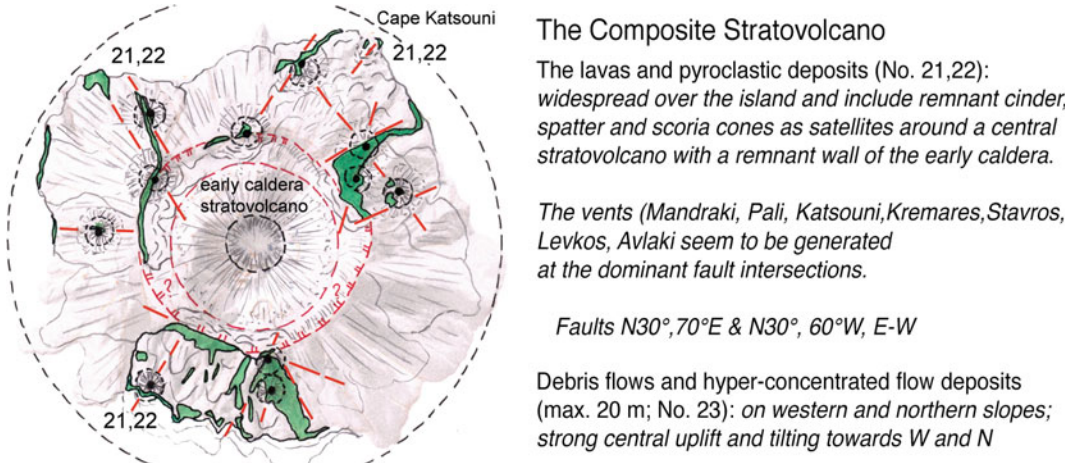

Fig. 3.33 The growth of a "Composite Stratovolcano" and distribution of small peripheral extrusive centers and flows

Fig. 3.34 The Kremares Cave at Cape Katsouni (NE corner of Nisyros). Basaltic andesite lava flow (unit No. 22) with red scoria sole and top above vent breccia (cave center) overlain by epiclastic debris flows (unit No. 23), "lower pumice" (unit No. 28), and "upper pumice" (unit No. 31) deposits. *Photo* V.J. Dietrich

Fig. 3.35 Ruins of Avlaki thermal bath; hot spring at sea level in the fault zone. Typical lava—pyroclastic succession (units Nos. 21 and 22) from a scoria cone in the southern slopes north of Avlaki. *Photo* V.J. Dietrich

deposits occur on western and northern slopes. The latter process also required strong central uplift and tilting towards W, NW and N, which also favored the formation of beach conglomerates (unit No. 23) at the north–western corner of the island.

Fig. 3.36 Planar-bedded surge deposits (unit No. 21, *dark-grey* layers) from an unknown source (e.g. tuff or scoria cone) overlain by epiclastic debris flows (unit No. 23, *top light-grey* blocky layer) and covered by a cap of "lower pumice" (unit No. 28, *orange*) and "upper pumice" (unit No. 31, *whitish*); in the northern slopes above Pali along the main road. *Photo* V.J. Dietrich

3.4.4 Terminal Cycle and Dome Collapse

The following volcanic cycle, subsequent to the stratovolcano cycles and after a significant period of dormant activity, can be bracketed by the appearance of epiclastic debris flows at its base and by the large « Loutra » debris avalanche as a result of a collapse of the northern caldera rim, probable at the end. These cycles differ from all previous volcanic cycles because of the dominance of their effusive eruption styles. Large volumes of differentiated lavas contributed to the filling of the northern sectors of the caldera and coverage of the northwestern and northern slopes of the island (Fig. 3.37). The cause of the dramatic change of the eruptive mode from all previous strombolian to sub-plinian explosive cycles to mainly effusive cycle is not clear, but it might be related to a sudden change in the geotectonic environment or to a major change in the magma reservoir.

Evidently, all lavas cover large portions of the upper slopes of the northern half of the island and may have derived from fissures and eruptive centers along a northern early caldera rim controlled by faults N30°E and N30–50°W generating intersections, thus extensional ways for magma emplacement. In addition, strong uplift of the central and south–eastern parts of the island is required to facilitate the east- and northward flow directions of all lavas. An associated process was the doming of dacitic magmas in the resurging caldera after the stratovolcano collapse.

During the first effusive cycle, a series of thin basaltic andesite-to-andesite lava flows with a total thickness of ca. 25 m (unit No. 24) was emitted from vents aligned along the early western caldera rim and covered the western slopes down to the sea. The second effusive cycle produced large volumes of dacitic lava flows with a thickness up 150 m, the "Emborio" lava dome and a neck (unit No. 25).

The time gap between the terminal caldera cycle and the collapse of the northern caldera rim is difficult to establish. The most plausible hypothesis favors a collapse after the emplacement of the voluminous dacitic lava flows. At the

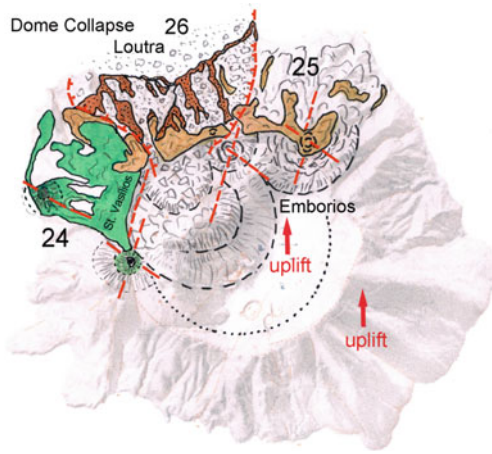

Terminal Cycle and Dome Collapse

Up to 10 basaltic andesite-to-andesite lava flows (No.24) on the western slopes (St. Vasilios) probably derived from vents on the western rim of the early caldera along faults N30°E & N60°W.

The up to 150m thick dacitic lava flows and Emborios lava dome (No.25) cover large portions of the upper slopes of the northern half of the island and may have derived from fissures along the northern early caldera rim at intersections of faults N30°E & N30-50°W.

The debris avalanche (No.26) covers the northern slopes from Mandraki to Pali (type locality "Loutra"), *interpreted as "dome collapse breccia" or break-off along intersections of faults N30°,70°E & N30°W.*

Fig. 3.37 Summary of the "Terminal Cycle and Dome Collapse"

Fig. 3.38 The "Emborio" dacitic lava dome and a neck (unit No. 25) forming the upper northern caldera wall between Mt. Akimaronas (453 m) and the village of Emborio. From *top* to *bottom* unit No. 25, Emborio dacitic lava; unit No. 15, andesitic lava; unit No. 14, dacitic lava rich in andesitic inclusions, unit No. 13, andesitic lava with red scoria sole; unit No. 11, pyroclastic sequence; unit No. 10, *thick* basaltic andesitic lava flow. *Photo* V.J. Dietrich

base of the chaotic collapse breccias, a 0.3–1 m horizon of dacitic ejecta with normal gradiation and fragments of dacitic lava have been observed in certain places. This deposit is interpreted as an indication of the start of a new cycle, emplacement of new magma from depth and bulging of high crustal levels.

The giant debris avalanche deposit (unit No. 26), named after the most diagnostic type locality "Loutra", reached variable thickness depending on the pre-existing morphology of the northern slopes between Mandraki and Pali (Figs. 3.37, 3.38, 3.39 and 3.40). The most characteristic megascopic feature of this large

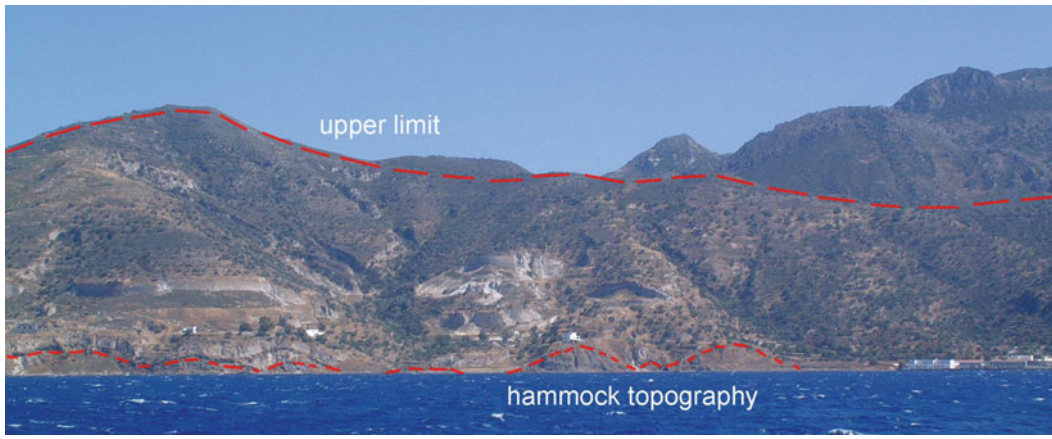

Fig. 3.39 The eastern part of the giant "Loutra debris avalanche": The "Loutra Bath" at the right side. The long hatched *red line* marks the *upper* limit of relict debris outcrops, whereas the short *stippled line* outlines the hammock topography at sea level. The hammocks are made of chaotic debris. *Photo* V.J. Dietrich

Fig. 3.40 "Loutra" debris avalanche east of Loutra. Compact block flow with little matrix support. Note that the smaller lithic components are partially rounded and thus may represent component of older volcanics and pyroclastics, e.g. reworked epiclastic deposits. *Photo* K. Kyriakopoulos

epiclastic unit is the hammocky topography, forming small hills of 20–30 m heights in the lower slopes along the shore. In fresh road cuts and in the cliffs along the shore, the chaotic internal structure of these unconsolidated deposits is evident. Fragments are mostly of dacitic composition, but rare pieces of andesites and red scoria from earlier strombolian eruptive cycles are also found.

An isolated andesitic lava flow, ~7–10 m in thickness (unit No. 27), appeared after the emplacement of the "Loutra" avalanche in the slopes of Loubounia (south of Loutra). It seems that the flow poured out of a fissure inside a scarp, produced by the Loutra avalanche. Apparently this flow marks the last andesitic eruption in the volcanic history of the island.

3.4.5 Caldera Eruptive Cycles and Caldera Collapse

A paleosol covers in many places the debris flows (unit No. 23), the dacitic lavas of Emborio (unit No. 25) and parts of the "Loutra" debris avalanche (unit No. 26). This is the indication that a large time interval and repose period occurred between the last dacitic and andesitic magmatic activity and the beginning of a major cycle of high explosive activity from highly differentiated rhyolitic magmas. During the "Caldera Eruptive Cycles", two vast successions of rhyolitic pumice derived from plinian eruptive cycles, designated as "lower and upper pumice", were deposited and divided by epiclastic deposits, the effusion of voluminous rhyolitic lava flows and the breakdown of a large caldera to the present day dimensions (Fig. 3.41). The lifetime of volcanic activity of each individual cycle, as well as of the total time-span is still not known, despite the occurrence of two widespread paleosols separating these two cycles, well exposed at Cape Katsouni (Fig. 3.42).

3.4.5.1 First Eruptive Cycle

The first voluminous (up 20–30 m thick) rhyolitic pyroclastic sequence, the "First Eruptive Cycle", designated as "lower pumice" (unit No. 28) resulted from a major plinian eruption and were deposited all over the island. Major occurrences are still present on the southern

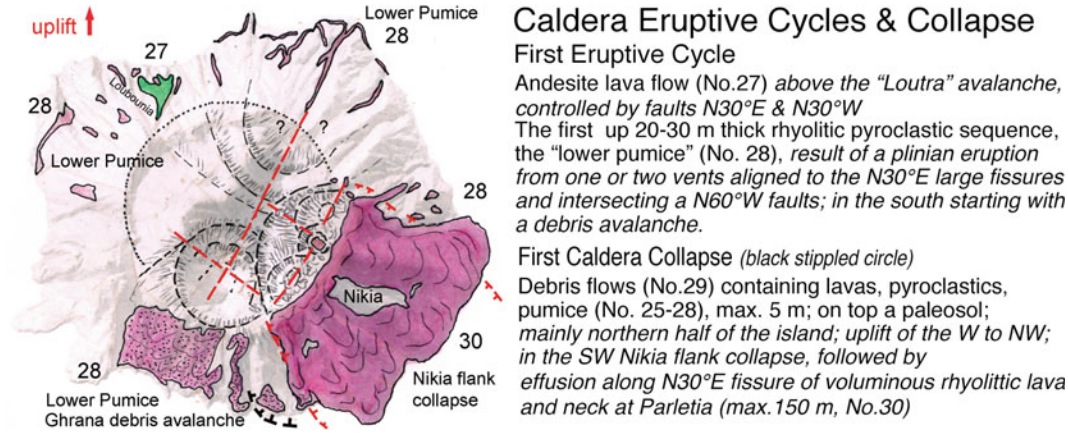

Fig. 3.41 Caldera cycles—Caldera collapse: first eruptive cycle combined with a first caldera collapse and SE flank collapse

Fig. 3.42 Lithostratigraphic pumice successions of the "Caldera Eruptive Cycles", the "Lower and Upper pumice" sequences, units Nos. 28 and 31 respectively at Cape Katsouni overlaying older lava (unit No. 20) and epiclastic (unit No. 23) deposits. *Photo* V.J. Dietrich

slopes, because of lack of coverage with younger pumice deposits (Fig. 3.41). However, no stratigraphic contacts occur to the northern and eastern equivalent of the "lower pumice units". Both are overlain by a paleosol and the large eastern rhyolitic lava flows (unit No. 30) of the second eruptive cycle.

Explosive phase

The explosive phase of the "lower pumice" LP can be divided into (1) in the lower part, plinian fall deposits, which contain lag breccias and up to 50% of lithics (some up to meter size) (unit No. 28a and b) and (2) in the upper part, poorly bedded fall layer with surges and pyroclastic flows (unit No. 28c). Both parts were probably deposited during one eruptive event since no major unconformity has been recognized within the deposits. The lithics include metamorphic limestones, skarns, hydrothermally altered rocks, unaltered volcanics and mafic cumulates, thus witnesses of a larger magma reservoir and an existing hydrothermal system. Yellowish weathering is a widespread feature within the "lower pumice". A chaotic debris-avalanche deposit has been recognized in the south–eastern coastal cliffs and along the beach at Ghrana bay over a distance of at least 500 m overlaying the basal pumice fallout flows indicating a southern slope failure during the initial phase of the first plinian fallout (Fig. 3.43).

Two eruption vents may have occurred in areas between the present southern and northeastern caldera rim aligned to a N30°E trending fissure and intersecting a N60°W faults (Fig. 3.41). The wide distribution of large fallout pumice blocks and lithic fragments, the presence of lag-breccias, poor bedding and sorting, as well as the greatest amount of fine-grained ash indicates proximal deposition in the southern part (Fig. 3.44a, b). In contrast, the plinian fallout of the northern part along the north and east cost exhibit more distal features (large lag breccia but thinner deposits, smaller diameters of pumice blocs and lapilli, sorting, reverse grading, and much lower lithic contents; Fig. 3.45). In addition, small ash- and mudflows occur.

The uneven areal distribution in grain size of the lower pumice pyroclastics on the island and the scarcity of the lower pumice deposits at the western half of the islands suggest an uplift of the western area during or shortly after the eruptive "lower pumice" cycle. Additional evidence of the uplift exists in the appearance of debris flows, mainly on the northern half of the island (unit No. 29), with components of lavas, pyroclastics and pumice (No. 25–28). All deposits are covered by a paleosol.

First Caldera Collapse

The "First Caldera Collapse" can only be estimated in space and time. We tend to place the collapse after the vast explosive phase. The highly differentiated rhyolitic magma may have been derived from rather shallow reservoirs in the upper crust (see later chapter of petrology and magma dynamics). As consequence of eruption the large volume deficiency could have generated a surficial depression and thus, initiated a first collapse that caused a first caldera. In addition, a major break in the steep morphology into two steps of the south–eastern caldera walls indicates

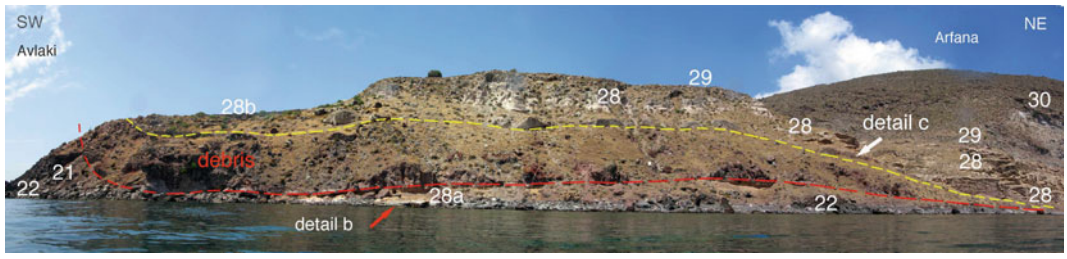

Fig. 3.43 "Lower pumice" (unit No. 28) deposits along the southeastern coast of Ghrana bay forming the base (*red arrow* and Fig. 3.75b in Electronic Supplementary Material Appendix 3) and top (*white arrow* and Fig. 3.75 c in Electronic Supplementary Material Appendix 3) of a coeval debris avalanche. *Photo* V.J. Dietrich

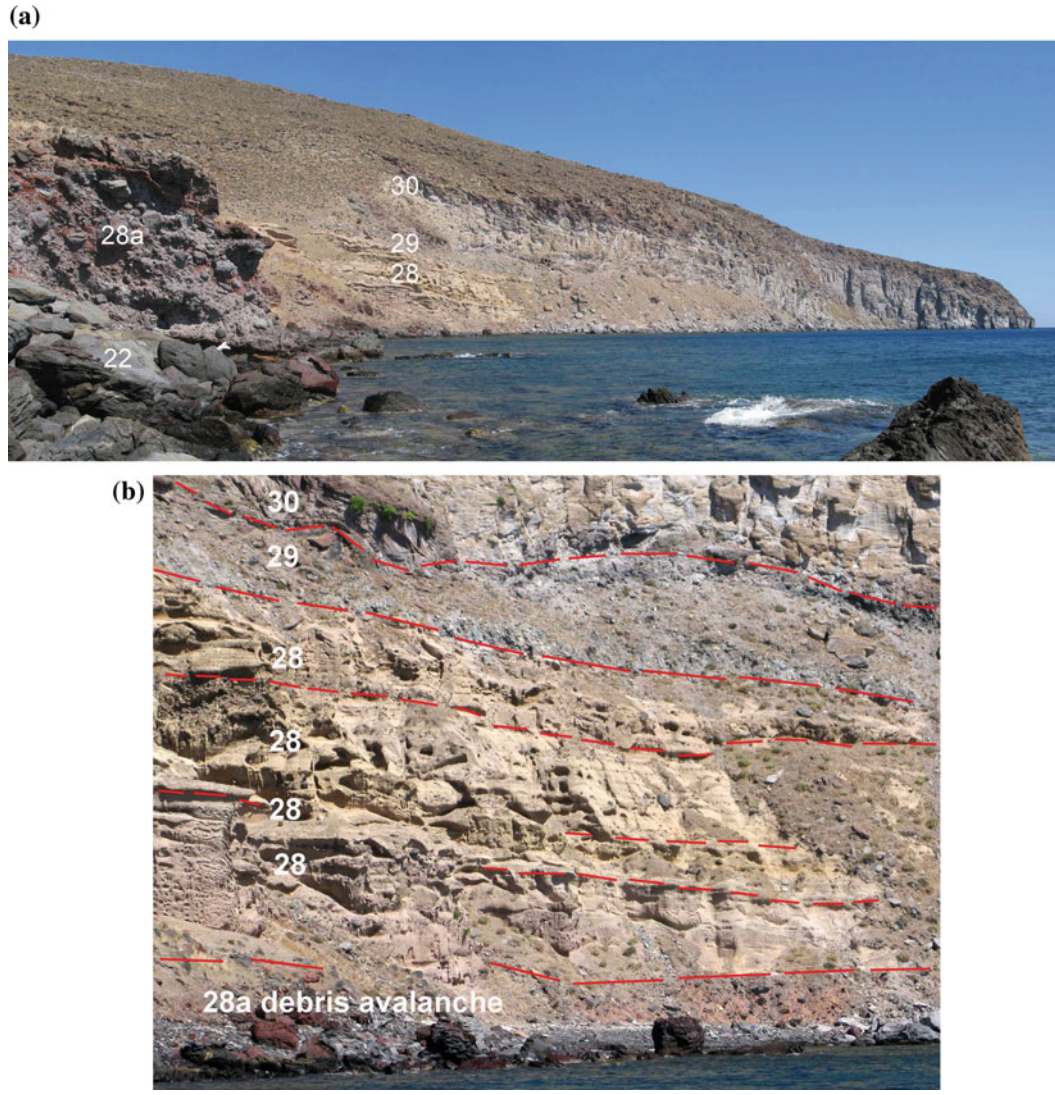

Fig. 3.44 **a** Debris avalanche (unit No. 28a) and "Lower pumice" succession (unit No. 28b, c) at the base of brecciated zone (unit No. 29) and rhyolithic lava (unit No. 30) in the southwestern flanks of Arfana, SW of Cape Avlaki. **b** Detail of (**a**) from *bottom* to *top*: (1) Debris-avalanche (unit No. 28a), (2) Lower pumice sequence (unit No. 28b, c) with intermediate lag breccia. (3) Heterogeneous breccia (unit No. 29) (4) Basal part of rhyolitic flow (unit No. 30) (5) Rhyolitic flow, unit No. 30. *Photo* V.J. Dietrich

a breakdown along slightly concentric normal N30°E striking fault before the extrusion of the rhyolitic flows (Fig. 3.41). The subsequent emplacement and doming of rhyolitic magma in the south–eastern part of the first caldera may have triggered a large flank collapse, ("Nikia Flank Collapse") and causing a major debris avalanche similar as the one on the northern half of the island ("Loutra" debris avalanche"). The voluminous rhyolitic lava flows do not flow into the caldera but into a major pre-existing south-east direction towards the sea.

The SE Nikia Flank Collapse

A major lateral collapse at the SE flank of Nisyros volcano (Fig. 3.46) has been recognized based on sea floor topography covered with

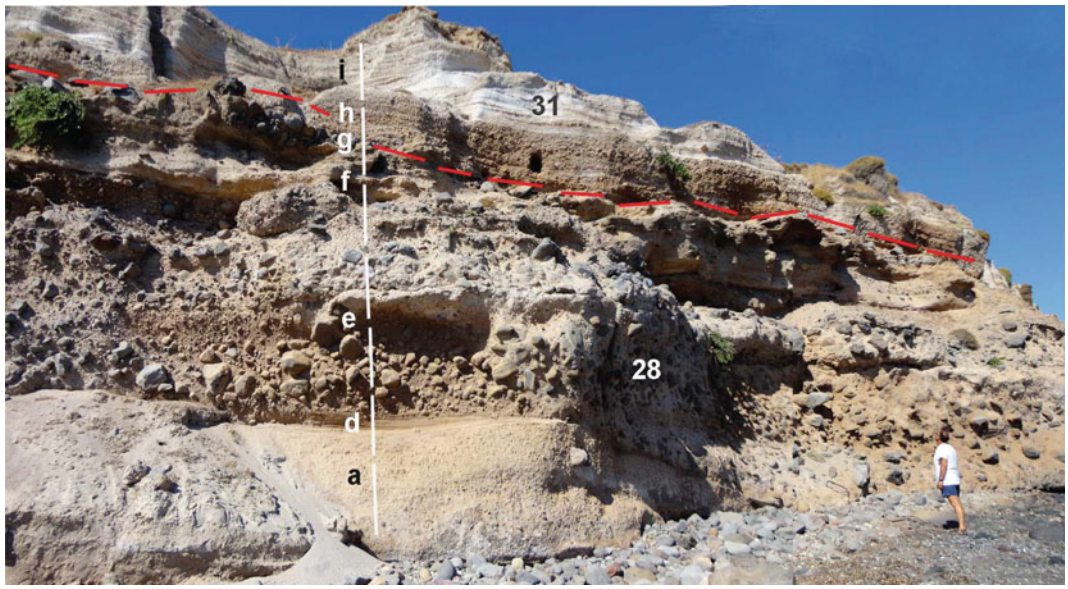

Fig. 3.45 Northern continuation of coastal profile at Louros Karanas (see Fig. 3.79a–c in Electronic Supplementary Material Appendix 3). Coarse blocky lag breccias between pyroclastic flows with matrix-rich pumice layers of the "Lower pumice" sequence (detailed description in Electronic Supplementary Material Appendix 3.3). *Photo* V.J. Dietrich

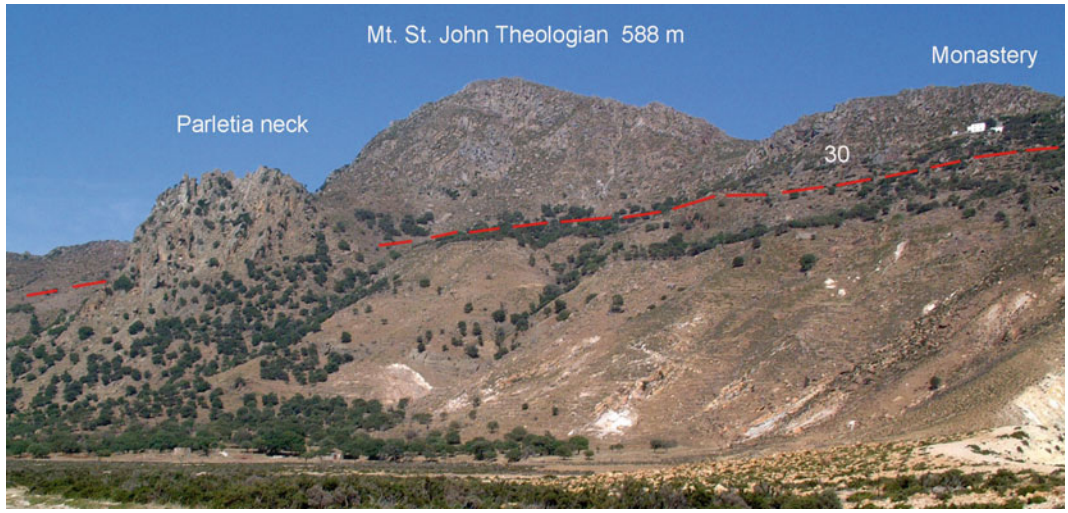

Fig. 3.46 Thick rhyolitic lava flows (unit No. 30) forming the eastern caldera rim with the highest elevation of Mt. St. John Theologian 589 m. In front *left* the rhyolitic Parletia neck (Medieval fort). Note the major break in the steep morphology into two steps of the south–eastern caldera walls, which indicates a breakdown along slightly concentric normal N30°E striking fault before the extrusion of the rhyolitic flows ("Nikia Flank Collapse"), limited to the north by the Parletia neck. *Photo* V. J. Dietrich

hammocks at a water depth of 250 and 380 m offshore the southeastern Nisyros flank. The large debris avalanche deposit covers an area of about 18 km^2 with a volume of about 1 km^3 and an average thickness of 40–50 m. The elongated hummocks show a fan-shaped distribution of

Fig. 3.47 Up bending rhyolitic flow front at Cape Avlaki. *Photo* V.J. Dietrich

their major axes with the apex pointing to the southeastern flank of Nisyros Island (Tibaldi et al. 2008; Nomikou et al. 2009). The evidence is based on multibeam data and lithoseismic profiles from the oceanographic research vessel "AEGAEO" of the H.C.M.R. The large debris avalanche deposit covers an area of about 18 km^2 with a volume of about 1 km^3 and an average thickness of 40–50 m.

Effusive phase

At least three major rhyolitic lava flows with a thickness up to 150 m and a total volume >1 km^3 (unit No. 30) represent a cycle during an extensive period of effusion (Fig. 3.41). A large morphological depression must have existed during that time in the southeastern part of the island since it facilitated the major flow directions towards southeast. The glass-rich, partly perlitic flows plunge down from the area in the present day eastern caldera walls between the Monastery Panaghia Kyra and the village of Nikia and enter the sea between the beach of Pachia Ammos and Avlaki (Fig. 3.47). Domes and a neck at Parletia piled up forming the eastern rim of the caldera. In several cases, the blocky surface of the flows is covered by a paleosol. The rhyolitic lava flows are younger than the plinian "lower pumice" deposits and older than the beginning of the second plinian eruptions of the "upper pumice". However, the time gap between these cycles remain unresolved up to now.

3.4.5.2 Second Eruptive Cycle

The palaeosol on top of the lower pumice forms a characteristic "marker horizon" between "lower and upper pumice" on the northern slopes of the volcano. However, the duration of this time gap is still not known. A debris flow (unit No. 29), containing components of lavas, pyroclastics and pumice of older units (units No. 23–26), with a maximum thickness between 5 and 20 m occurs along the northern coast close to the little harbour of Loutrà.

The first volcanic phase of the "Second Eruptive Cycle" (Fig. 3.48) is not well documented. Only one outcrop (at the base of the Nikia lava), a 1 m thick fallout horizon occurs above the "lower pumice", which consists of lapilli and blocks of slightly vesicular perlitic obsidian, indicating an explosive beginning before the effusion and emplacement of the major rhyolitic lava flow on top.

Explosive phase

The climactic explosive cycle produced an up to 60 m thick rhyolitic pyroclastic sequence, the "upper pumice" UP (unit No. 31) with a

fall-surge-flow-surge sequence, which has been deposited all over the island (Fig. 3.48). Major occurrences lie between Loutrà, Pali and Cape Katsouni in the northern and northeastern slopes of the island (Figs. 3.49 and 3.50). Smaller occurrences exist on the SE slopes, on the Nikia rhyolite. Deposits have not been found in the western and southern part of the island.

The proximal-to-distal transition in these bedforms may result from cooling of hot, dry steam propelled surges with condensation of water in the more distal zones (Limburg and Varekamp 1991). Water condensation caused the formation of accretionary lapilli and accelerated rates of deposition of fines, leading to thicker deposits and climbing ripple sets

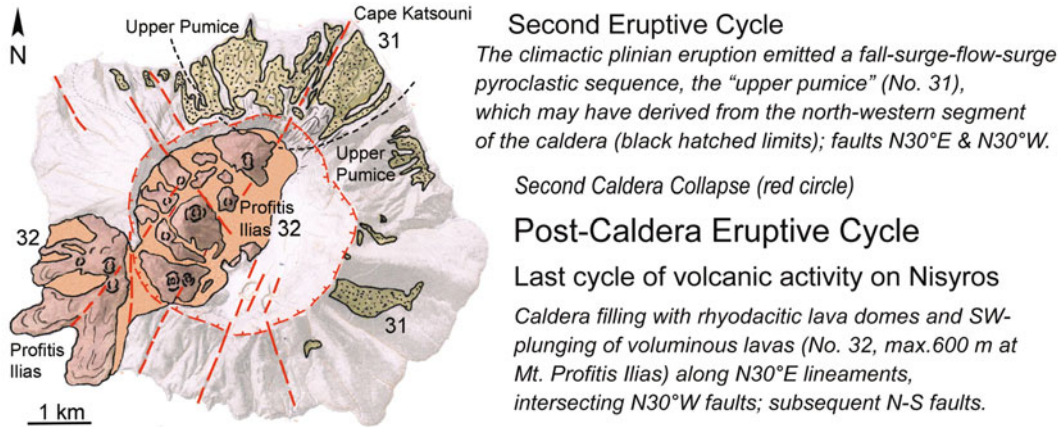

Fig. 3.48 Second eruptive cycle and second caldera collapse; the last cycle of volcanic activity on Nisyros

Fig. 3.49 Upper pumice pyroclastic sequence, unit No. 31 with max. 60 m total *thickness*. North–east coast between Plomos and Cape Katsouni. The numbers refer to the generalised tephrostratigraphic succession; detailed stratigraphic description in Electronic Supplementary Material Appendix 3.3. *Photo* V.J. Dietrich

Fig. 3.50 "Upper pumice" unit No. 31a at Plomos. Beginning with plinian pumice fall and wavy surge, then continuation with pyroclastic block flow (6–20 m *thickness*). *Photo* V. J. Dietrich

(Fig. 3.50). The upper units were deposited as non-turbulent pyroclastic flows with massive bedding, but absence of grading and stratification. They also contain lithic-rich layers and in the northeast coastal deposits several wavy surge layers. The upper part of the eruptive cycle represents a sequence massive surge deposits with extreme fragmentation, may be the result of water-magma interaction (Fig. 3.51).

The eruption centre of the "second eruptive cycle" may have occurred in the north–western segment of the caldera, controlled by intersecting fault zones N30°E and N30°W (Fig. 3.48), since the distribution of the maximum thickness of the fallout as well the pumice bomb and lithic last size clast sizes point towards the north–western and northern half of the island.

Limburg and Varekamp (1991) recognized a progress in the degree of hydrothermal alteration in the lithics from the lower part to the upper part of the entire succession. The temperatures of hydrothermal alteration, according to the mineral assemblages in the lithics start from 70–150 °C (argillite chunks) to >350 °C in epidote and diopside bearing skarns. This is in accordance with temperatures encountered in the geothermal drill holes NIS 1 and 2 below the caldera floor between 1000 and 1880 m depth (Barberi et al. 1988).

Erupted volume and plume shape

A first attempt to estimate the erupted volumes during the "Caldera Eruptive Cycles" was given by Limburg and Varekamp (1991). Isopach and isopleth patterns were derived from of the thickness distribution of the plinian eruptive sequences of both, the first and the second eruptive cycles. For the second plinian eruptive cycle, an 8 m average thickness at the source and a 7 cm thickness at 120 km distance

Fig. 3.51 Upper pumice (unit No. 31) south above Cape Katsouni. The succession is composed of ash flow deposits and planar-bedded surges in the *upper part*. The upper most sequence (*orange colors*) consists mainly of planar-bedded surges. *Photo* K. Kyriakopoulos

(Vinci 1983) was assumed. Using a model with circular isopachs and exponential thickness decay, the calculation showed an upper volume of 32 km^3, which is equivalent to a DRE ("Dry Rock Equivalent") of 10 km^3. The more realistic approach, using an elliptical distribution of isopachs reduced roughly the volume by the factor 4, which means a volume of 2–3 km^3. A crude volume calculation of the caldera before infill of ca. 100 m of talus and alluvial deposits yielded a maximum of extracted volume of 5 km^3. The approximate half-width of 1.9 km and a height of 15 km for the column during the plinian phase at minimum cross-wind was calculated using the 7 cm lithic isopleth distribution. A maximum column height of 20 km was estimated from the shape of the isopleth and isopach pattern. Longchamp et al. (2011) derived an "erupted volume for the south vent (considered as the best vent location) ranges between 2 and 27 $x10^8$ m^3 for the LP and between 1 and 5 $x10^8$ m^3 for the UP based on the application of four different methods (integration of exponential fit based on one isopach line, integration of exponential and power-law fit based on two isopach lines, and an inversion technique combined with an advection-diffusion model)".

The second Caldera collapse

During both eruptive cycles, large volumes of similar magnitudes of highly differentiated magmas were discharged. According to the lithics (composition, metamorphic state (Limburg and Varekamp 1991), they originated from magma reservoirs at high crustal levels. The mass deficiency after each eruptive cycle must necessarily have caused an internal collapse of the central part of the island and formation of the caldera structure. The first eruptive cycle was possibly followed by a first caldera collapse. The second caldera collapse must have happened in a very similar way. The possible evidence for such a situation is found in the hydrothermally altered clay chunks as part of the first caldera alluvial beds in the lower fall-flow sequence of the second eruptive cycle. However, the first caldera must have had a smaller diameter than the present day one, which formats the present day state.

3.4.6 Post-caldera Eruptive Cycle

The post-caldera rhyodacitic lava domes comprise six groups of endogenous domes and with light gray perlitic lava flows originating from them

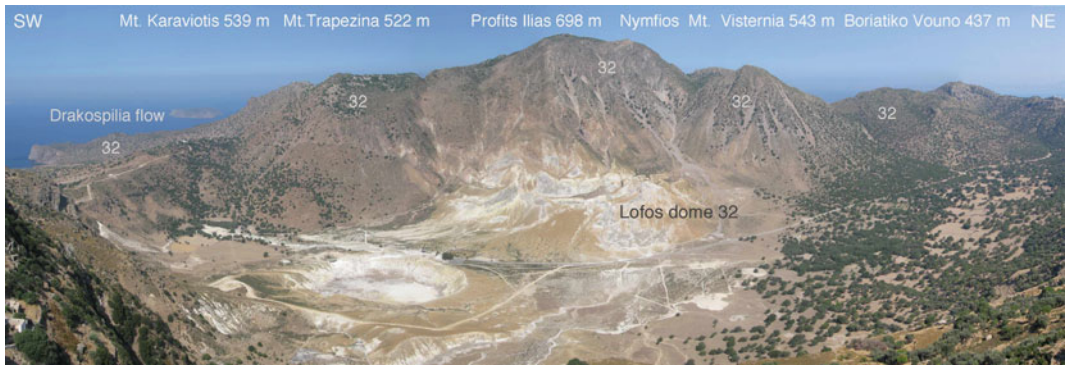

Fig. 3.52 The Nisyros caldera with the hydrothermal explosion crater field surrounded by rhyodacitic domes (from *left* to *right*), Mt. Karaviotis, Mt. Trapezina, Profitis Ilias, Nymfios, Mt. Visternia, Lofos dome, and Mt. Boriatiko Vouno. *Photo* V.J. Dietrich

(unit No. 32). They fill up the western half of the caldera with a max. thickness of 600 m and seem to be aligned along three parallel 30°NE trending fissure zones intersecting several N30°W fault zones (Figs. 3.48 and 3.52). They were emitted during the last eruptive cycle of Nisyros volcano during purely effusive phases and lack any sign of explosive precursors. The domes are: Mt. Profitis Ilias (698 m), Boriatiko Vouno (437 m), Nymfios, Visternia, Dhiavatis, Trapezina, and Karaviotis (539 m). In addition, a small dome (Lofos, 214 m) is found in the southeastern edge, which has been devastated by recent hydrothermal explosions and fumarolic activity. All domes can be subdivided into four older central groups, Dhiavatis—Profitis Ilias, Nymfios, Visternia, Trapezina, and Lofos and two much younger domes, Boriatiko Vouno in the Northeast and Karaviotis with the silicic flow lobes of Kateros, Kilia, and Drakospilia in the Southwest. They exhibit steep spines and scoria at the surface, as well as they lack soil deposits and minor proximal scree deposits.

3.5 Geochronology

Geochronological data of volcanic rocks and soils from Nisyros Island and the Kos-Yali-Nisyros Volcanic Field are relatively few. During the past 40 years numerous attempts have been undertaken, however without consistent and conclusive results in most cases. Earlier data are controversial and accompanied with large errors (Table 3.2). The following methods have been applied:

- ^{14}C fission track analysis on obsidian glass,
- K–Ar on whole rock and volcanic glass,
- $^{40}Ar/^{39}Ar$ on feldspars, and
- U–Th disequilibrium measurements on paleosols sandwiched between volcanic and pyroclastics, the latter discussed in Büttner et al. (2005),
- Th/U measurements on whole rocks and zircon and Pb–U dating on zircon using laser ablation inductively coupled plasma mass spectrometry (LA–ICP–MS, Guillong et al. 2014).

Reliable age determinations with the $^{40}Ar/^{39}Ar$ method have been obtained from the Kos Plateau Tuff (KPT) with 161 ± 1 and 166 ± 2 ka (Smith et al. 1996; Bachmann et al. 2010). The new Pb–U ages of the youngest zircons (Guillong et al. 2014) measured from the Nisyros silicic volcanics provide the first geochronological estimates, which are in accordance with the established lithostratigraphy and interpreted as maximum ages of their eruption: The Lower Pumice with 124 ± 35 ka (unit No. 28), the Nikia rhyolite flows with 111 ± 42 ka (unit No. 30), and the upper Pumice with 70 ± 35 ka (unit No. 31). The K–Ar data of 66 ± 2 and 24 ka on fission track (Table 3.1) are of restricted geological meaning.

Table 3.2 Geochronological data of volcanic rocks and soils from Nisyros Island and Kos Plateau Tuff (KPT); *SHRIMP* sensitive high resolution ion microprobe, *ID–TIMS* isotope-dilution thermal ionization mass spectrometry

Lithostratigraphic unit	Age	Method	Reference
Yali obsidian	24 ka	Fission track on glass	Wagner et al. (1976)
Yali pumice (No. 33)	31 ka	Oxygen isotope stratigr.	Federmann and Carey (1980)
Upper pumice (No. 31)	>44 ka	^{14}C	Limburg & Varekamp (1991)
Upper pumice (? No. 31)	110 ± 40 ka	Fission track on glass	Barberi et al. (1988)
Upper pumice (? No. 31)	24 ka	Sediment, rate, extrapol.	Vinci (1985)
Upper pumice (No. 31)	**70 ± 35 ka**	LA-ICP-MS Pb–U, zircon	Guillong et al. (2014)
Nikia Rhyolite (No. 30)	**111 ± 42 ka**	LA-ICP-MS Pb–U, zircon	Guillong et al. (2014)
Lower pumice (No. 28)	**124 ± 35 ka**	LA-ICP-MS Pb–U on zircon	Guillong et al. (2014)
Lower pumice (No. 28)	35 ka	Sediment, rate, extrapol.	Hardimann (1999)
Paleosol (? No. 21)	24.26 ± 0.56	^{14}C on charcoal	Rehren (1988)
Dacite Afionas (No. 18)	37 ± 24 ka	K–Ar on plagioclase	Rehren (1988)
Dacite Afionas (No. 18)	39 ± 26 ka	K–Ar on groundmass	Rehren (1988)
Rhyolite Argos (No. 17)	66.6 ± 2 ka	K–Ar on plagioclase	Keller et al. (1990)
Rhyolite Argos (? No. 17)	200 ± 50	K–Ar on bulk rock	Di Paola (1974)
Andesite (? No. 24)	100 ± 100	K–Ar on bulk rock	Matsuda et al. (1999)
Andesite (? No. 1)	800 + 700	K–Ar on bulk rock	Matsuda et al. (1999)
Kos Plateau Tuff (KPT)	**161 ± 1 ka**	$^{40}Ar/^{39}Ar$ on sanidine	Smith et al. (1996)
Kos Plateau Tuff (KPT)	**166 ± 2 ka**	$^{40}Ar/^{39}Ar$ on sanidine	Bachmann et al. (2010)
Kos Plateau Tuff (KPT)	**160 ± 2 ka**	SHRIMP, LA-ICP-MS, ID-TIMS	Guillong et al. (2014)

Some of the major reasons for the lack of accurate geochronological data are as follows:

- The rarity of sanidine and biotite in the evolved rocks of Nisyros volcano do not permit high-precision Ar/Ar analyses. Low-K Amphibole and plagioclase crystals do not provide reliable ages for such young systems, and glass (where most of the potassium is) is typically unreliable (hydration, alteration).
- ^{14}C analysis in soils, charcoal and paleosols on Nisyros Island may be contaminated by the strong CO_2 degassing all over the volcano (in the order over 1000 tons/day, see Chap. 5).

Future age determination studies using LA-ICP-MS U/Pb dating on single zircon crystals may help resolving some of these issues.

References

Allen SR (2001) Reconstruction of a major caldera-forming eruption from pyroclastic deposit characteristics: Kos Plateau Tuff eastern Aegean Sea. J Volcanol Geotherm Res 105:141–162

Bachmann O (2010) The petrologic evolution and pre-eruptive conditions of the rhyolitic Kos Plateau Tuff (Aegean Arc). Cent Europ J Geosci. doi:10.2478/v10085-010-0009-4

Barberi F, Navarro JM, Rosi M, Santacroce R, Sbrana A (1988) Explosive interaction of magma with ground water: insights from xenoliths and geothermal drillings. Rend Soc Ital Mineral Petrol 43:901–926

Buettner A, Kleinhanns IC, Rufer D, Hunziker JC, Villa IM (2005) Magma generation at the easternmost section of the Hellenic Arc: Hf, Nd, Pb and Sr isotope geochemistry of Nisyros and Yali volcanoes (Greece). Lithos 83:29–46

Davis EN (1967) Zur Geologie und Petrologie des Inseln Nisyros und Jali (Dodecanese). Praktika Akademy of Athens 42:235–252

De Goer de Herve A (2008) Chapter 5, Peperites from the Limagne Trench (Auvergne, French Massif Central), a distinctive feature of phreatomagmatic pyroclastics. History of semantic drift. In: Leyrit H, Montenat C (eds) Volcaniclastic rocks, from magmas to sediments. Taylor Francis, 270 p

Desio A (1931) Le Isole Italiane dell'Egeo—Studi geologici e geografici-fisici. Mem descrittive della Carta Geologica d'Italia. R. Ufficia Geologica d'Italia

Di Paola GM (1974) Volcanology and petrology of Nisyros Island (Dodecanese Greece). Bull Volcanol 38:944–987

Drakopoulos J, Delibasis N (1982) The focal mechanism of earthquakes in the major area of Greece for the period 1947–1981. Univ of Athens Seismological Laboratory No. 2

Federman AN, Carey SN (1980) Electron microprobe correlation of tephra layers from Eastern Mediterranean abyssal sediments and the Island of Santorini. Quatern Res 13:160–171

Geotermica Italiana (1983) Nisyros 1 geothermal well PPC-EEC report, pp 1–106

Geotermica Italiana (1984) Nisyros 2 geothermal well PPC-EEC report, pp 1–44

GEOWARN (2003) GEOWARN Geo-spatial warning system—synthesis report GEOWARN consortium Athens (Greece) and Zurich (Switzerland), p 57 (http://www.geowarnorg)

Guillong M, von Quadt A, Sakata S, Peytcheva I, Bachmann O (2014) LA–ICP–MS Pb–U dating of young zircons from the Kos-Nisyros volcanic centre SE Aegean arc. J Anal At Spectrum 29:963–970

Hardimann JC (1999) Deep sea tephra from Nisyros Island eastern Aegean Sea Greece. In: Firth CR, McGuire WJ (eds) Volcanoes in the Quaternary, vol 161. Geological Society of Special Publication London, pp 69–88

Hildreth W S (2007) Quaternary magmatism in the cascades- geological perspectives. US Geological Survey Professional Paper 1744, p 125

Keller J, Rehren Th, Stadlbauer E (1990) Explosive volcanism in the Hellenic Arc; a summary and review. In: Hardy DA, Keller J, Galanopoulos VP, Flemming NC, Druitt TH (eds) Thera and the Aegean World III proceedings of the third international congress The Thera Foundation London, vol 2, pp 13–26

Limburg EM, Varekamp JC (1991) Young pumice deposits on Nisyros Greece. Bull Volcanol 54:68–77

Longchamp C, Bonadonna C, Bachmann O, Skopelitis A (2011) Characterization of tephra deposits with limited exposure: the example of the two largest explosive eruptions at Nisyros volcano (Greece). B Volcanol 73:1337-1352

Makris J, Stobbe C (1984) Physical properties and state of the crust and upper mantle of the Eastern Mediterranean Sea deduced from geophysical data. Mar Geol 55:347–363

Martelli A (1917) Il gruppo eruttivo di Nisiro nel mare Egeo. Mem Mat Fis Soc Ital Sc (detta dei XL) Serie 3a Tome 20:79–167

Matsuda J-I, Senoh K, Maruoka T, Sato H, Mitropoulos P (1999) K–Ar ages of the Aegean volcanic rocks and their implications for the arc–trench system. Geochem J 33:369–377

Nomikou P, Papanikolaou D (2000) Active geodynamics at Nisyros the eastern edge of the Aegean Volcanic Arc: emphasis on submarine surveys. In: Proceedings of the 3rd international conference on geology East Mediterranean, Sept 1998, pp 97–103

Nomikou P, Papanikolaou D (2011) Extension of active fault zones on Nisyros Volcano across the Yali-Nisyros Channel based on Onshore and Offshore data. Mar Geophys Res Spec Issue Seafloor Map Geohaz Assess. doi:10.1007/s11001-011-9119-z

Nomikou P, Tibaldi A, Pasquare F, Papanikolaou D (2009) Submarine morphological analysis based on multibeam data of a huge collapse at the SE flank of Nisyros volcano. In: International conference on seafloor mapping for geohazard assesment 11–13 May, Ischia Italy Rend Soc Geol It, vol 7, pp 177–179

Papanikolaou DJ, Lekkas EL, Sakelariou DT (1991) Geological structure and evolution of Nisyros volcano. Bull Geol Soc Greece 25:405–419

Rehren TH (1988) Geochemie und petrologie von Nisyros (Oestliche Agais). PhD Thesis Univ Freiburg

Skilling IP, White JDL, McPhie J (2002) Peperite: a review of magma-sediment mingling. J Volcanol Geotherm Res 114:1–17

Smith PE, York D, Chen Y, Evensen NM (1996) Single crystal $^{40}Ar/^{39}Ar$ dating of a late quaternary paroxysm on Kos Greece; concordance of terrestrial and marine ages. Geophys Res Lett 23:3047–3050

Stadlbauer E (1988) Vulkanologisch-geochemische Analyse eines jungen Ignimbrits: der Kos-Plateau-Tuff (Südost-Ägäis) PhD Thesis. Albert-Ludwigs-Universität Freiburg im Breisgau, 184 p

Tibaldi A, Pasquarè FA, Papanikolaou D, Nomikou P (2008) Discovery of a huge sector collapse at the Nisyros volcano Greece by on-land and offshore geological-structural data. J Volcanol Geotherm Res 177:485–499

Vinci A (1983) A new ash layer "Nisyros layer" in the Aegean sea sediments. Boll Oceanol Teor Appl 1:341–342

Vinci A (1985) Distribution and chemical composition of tephra layers from Eastern Mediterranean abyssal sediments. Mar Geol 64:143–155

Volentik A, Vanderkluysen L, Principe C, Hunziker JC (2005) Stratigraphy of Nisyros vollcano (Greece). In: Hunziker JC, Marini L (eds) The petrology and geochemistry of lavas and tephras of Nisyros Volcano (Greece), vol 44. Mém Géologie (Lausanne), pp 26–66

Volentik A, Vanderkluysen L, Principe C (2002) Stratigraphy of the Caldera walls of Nisyros volcano Greece. Eclogae Geol Helv 95:223–235

Vougioukalakis G (1993) Volcanic stratigraphy and evolution of Nisyros Island. Bull Geol Soc Greece 28:239–258

Vougioukalakis GE (1998) Blue volcanoes: Nisyros Nisyros. Regional Council Mandraki, p 78

Vougioukalakis G (2003) Nisyros sheet, geological map of Greece 1:25,000 IGME Institute of Geology Mineral Exploration, Athens Greece

Wagner GJ, Storzer D, Keller J (1976) Spaltspurendatierungen quartarer Gesteinsglaser aus dem Mittelmeerraum. N Jb Miner Mh 2:84–94